



**VAAL UNIVERSITY  
OF TECHNOLOGY**

*Inspiring thought. Shaping talent.  
Inspiring thought. Shaping talent.*

# **Application of neural network techniques to predict the heavy metals in acid mine drainage from South African mines**

Dissertation submitted in fulfilment of the requirements for the degree

Master of Engineering: Chemical

In the Faculty of Engineering and Technology

Department of Chemical Engineering

**ANDANI VALENTIA MALIEHE**

(Bachelor of Technology: Chemical Engineering)

Student number: 213021854

Supervisor: Prof. John Kabuba Tshilenge

Co-Supervisor: Prof. P. Osifo and Dr. H. Matjie

(April, 2022)

## Declaration

I, **MALIEHE ANDANI VALENTIA**, declare that this thesis is my original work and that it has not been presented to any other university or institution for similar or any other degree award.

.....  
Signature

.....  
Date

## Acknowledgements

I would like to extend my gratitude to the institution of the Vaal University of Technology and the university library for providing me with the resources for my research.

I would like to extend my gratitude to The Petroleum Agency (Upstream Training Trust) who funded me during my degree.

Special thanks to my parents, Mr Itani and Mrs Nkhesani Maliehe for their encouragement and continued support as well as funding. My siblings, Livhuwani and Dakalo, thank you for your support during my research.

I appreciate the help of my supervisor, Dr. Kabuba Tshilenge and co-supervisors, Prof. P. Osifo and Dr. H. Matjie for their support, guidance and encouragement.

I would also like to acknowledge Sibanye Western Basin Acid Mine Drainage Plant for their assistance in sample taking, and Setpoint laboratories for their assistance in analyzing samples.

My sincere appreciation to my entire family, friends and colleagues for their love, assistance, and support during this journey. It has truly been an honour working with you and learning from you. And finally, I would like to thank God for his grace during this journey.

## **Dedication**

I would like to dedicate this dissertation to my family, Mr Itani and Mrs Nkhesani Maliehe, my loving and caring parents, as well as my supportive siblings, Livhuwani and Dakalo Maliehe.



## Abstract

Acid mine drainage (AMD) refers to acidic water generated during mining activities and is characterised by a low pH, high salt content, and the presence of heavy metals. To treat water sources contaminated with AMD, sampling and laboratory analysis will have to be done for each water source to determine the concentrations of heavy metals. This process is time-consuming, high in cost and may involve human error or negligence.

The application of neural network (NN) techniques to predict the heavy metals in AMD from South African mines has been presented. Four specific objectives were pursued in this dissertation. The first one was to identify AMD and analyse for heavy metals in the AMD. Heavy metals that were identified and found to be in high concentrations in the AMD sample from Sibanye Western Basin AMD Treatment Plant are Zn, Fe, Mn, Si, and Ni. The other objectives of the study were to determine the input, output, and hidden layers of the NN structure (application of NN); (2) to find the appropriate algorithm to train the NN, and to compare the NN results (outputs) with the measured concentrations of major heavy metals sampled (targets).

The Backpropagation Neural Network (BPNN) model had three layers which included the input layer (pH,  $\text{SO}_4^{2-}$ , and TDS), the hidden layer (five neurons) with a tangent sigmoid transfer function (*tansig*) and the output layer (Cu, Fe, Mn, and Zn) with linear transfer function (*purelin*). The predictions for heavy metals (Zn, Fe, Mn, Si, and Ni) using the NN method focusing on a BP forward pass (feed-forward backpropagation NN) with ten different algorithms were presented and compared with the measured data. The mean square error (MSE) value was calculated for ten algorithms and compared to identify the one that is most appropriate for the prediction process and the model by having the lowest value. It was determined that the Levenberg-Marquardt back-propagation (*trainlm*) algorithm resulted in the best fitting during training because it resulted in an MSE value of 0.00041, meaning the error was very low when this algorithm was used.

## **Publications and conference presentations**

Journal article: Kabuba, J. & Maliehe, A.V., 2021. Application of neural network techniques to predict the heavy metals in acid mine drainage from South African mines. *Water, Air, and Soil Pollution*, pp. 01-12.

This journal is based on chapters 1 to 5 of the dissertation and was submitted for possible publication in *Water, Air, and Soil Pollution* and the submission number is WATE-S-21-01406. This journal was not accepted for publishing.

Journal article: Kabuba, J. & Maliehe, A.V., 2021. Application of neural network techniques to predict the heavy metals in acid mine drainage from South African mines. *Water Science and Technology*, pp. 01-12.

Based on chapters 1 to 5 of the dissertation the journal has been accepted and published in *Water Science and Technology* with the number WST-EM211089.

## ***TABLE OF CONTENTS***

<b>Declaration.....</b>	<b>i</b>
<b>Acknowledgements .....</b>	<b>ii</b>
<b>Dedication .....</b>	<b>iii</b>
<b>Abstract.....</b>	<b>iv</b>
<b>Publications and conference presentations.....</b>	<b>v</b>
<b>Acronyms and abbreviations .....</b>	<b>vi</b>
<b>Glossary .....</b>	<b>ix</b>
<b>Chapter 1: Introduction .....</b>	<b>1</b>
<b>1.1 Background of the study .....</b>	<b>1</b>
<b>1.2 Motivation.....</b>	<b>4</b>
<b>1.3 Problem statement .....</b>	<b>5</b>
<b>1.4. Objective .....</b>	<b>5</b>
<b>1.4.1 Specific objectives .....</b>	<b>5</b>
<b>1.5 Outline of dissertation .....</b>	<b>6</b>
<b>Chapter 2: Literature Review .....</b>	<b>8</b>
<b>2.1 Introduction.....</b>	<b>8</b>
<b>2.2 Sources and Formation of AMD.....</b>	<b>8</b>
<b>2.3 Acid Mine Drainage and Heavy Metals .....</b>	<b>10</b>
<b>2.4 AMD Treatment Methods.....</b>	<b>14</b>
<b>2.5 Application of Neural Network.....</b>	<b>20</b>
<b>Chapter Summary .....</b>	<b>31</b>
<b>Chapter 3: methodology .....</b>	<b>32</b>
<b>3.1 Materials and Chemicals.....</b>	<b>32</b>
<b>3.2. Experimental Procedure .....</b>	<b>32</b>
<b>3.2.1 Site Identification and Sampling Procedure.....</b>	<b>33</b>
<b>3.2.2 Neural Network Procedure .....</b>	<b>37</b>
<b>Chapter Summary .....</b>	<b>39</b>

<b>Chapter 4: Results and discussion.....</b>	<b>40</b>
<b>4.1 Identification of AMD and analysis of raw AMD and treated AMD samples .....</b>	<b>40</b>
<b>4.2 Application of NN .....</b>	<b>46</b>
<b>4.2.1 Selection of the BP Training Algorithm.....</b>	<b>46</b>
<b>4.2.2 Data Distribution .....</b>	<b>47</b>
<b>4.2.3 Selection of NN Structure.....</b>	<b>58</b>
<b>4.2.4 Selection of Initial Weight .....</b>	<b>59</b>
<b>Chapter Summary .....</b>	<b>60</b>
<b>chapter 5: conclusions and recommendations.....</b>	<b>61</b>
<b>5.1 Conclusions.....</b>	<b>61</b>
<b>5.2 Recommendations .....</b>	<b>61</b>
<b>References.....</b>	<b>63</b>
<b>Appendix A.....</b>	<b>69</b>



## List of figures

Figure 1: Image of a typical neuron (Rooki et al., 2011).....	21
Figure 2: A single-layer feed-forward NN (Sazli, 2006).....	22
Figure 3: A multi-layer feed-forward NN (Sazli, 2006).....	23
Figure 4: Diagram indicating the flow of the experimental process.....	32
Figure 5: Map of the Sibanye Western Basin AMD Plant in Randfontein.....	33
Figure 6: Satellite representation of the Sibanye Western Basin AMD Plant in Randfontein map .....	34
Figure 7: Images of raw and neutralised samples from AMD treatment plant.....	35
Figure 8: Training, validation, and test MSE for the LMA for the Batch gradient descent (traingd) algorithm.....	48
Figure 9: Training, validation, and test MSE for the LMA for the Batch gradient descent with momentum (traingdm) algorithm.....	49
Figure 10: Training, validation, and test MSE for the BFGS quasi-Newton back-propagation (trainbfg) LMA for the algorithm.....	50
Figure 11: Training, validation, and test MSE for the LMA for the Fletcher-Reeves conjugate gradient back-propagation (traincgf) algorithm.....	51
Figure 12: Training, validation, and test MSE for the LMA for the One step secant back- propagation (trainoss) algorithm.....	52
Figure 13: Training, validation, and test MSE for the LMA for the Polak-Ribiere conjugate gradient back-propagation (traincgp) algorithm.....	53
Figure 14: Training, validation, and test MSE for the LMA for the Powell-Beale conjugate gradient back-propagation (traincgb) algorithm.....	54
Figure 15: Training, validation, and test MSE for the LMA for the Scaled conjugate gradient back-propagation (trainscg) algorithm.....	55
Figure 16: Training, validation, and test MSE for the LMA for the Variable learning rate back- propagation (traingdx) algorithm.....	56
Figure 17: Training, validation, and test MSE for the LMA for the Levenberg-Marquardt back- propagation (trainlm) algorithm.....	57
Figure 18: Optimal NN structure from MATLAB NNtool.....	58
Figure 19: Detailed optimal NN structure using the trainlm BP algorithm.....	58

## List of tables

Table 1: Summary of some research done on NN technology by different authors.....	29
Table 2: Water characteristics analysis results for AMD (raw and treated) at Sibanye Western Basin AMD Plant.....	41
Table 3: Heavy metal analysis results for AMD (raw and treated) at Sibanye Western Basin AMD Plant.....	43
Table 4: Heavy metal analysis results for AMD (raw and treated) at Sibanye Western Basin AMD Plant.....	45
Table 5: Comparison of 10 BP algorithms .....	46



## Acronyms and Abbreviations

<b>Al</b>	Aluminium
<b>AMD</b>	Acid Mine Drainage
<b>APP</b>	Aquifer Protection Permit
<b>As</b>	Arsenic
<b>BPNN</b>	Backpropagation Neural Network
<b>Ca(OH)<sub>2</sub></b>	Calcium Hydroxide also known as Slacked Lime
<b>CaCO<sub>3</sub></b>	Calcium Carbonate also known as Limestone
<b>CaC<sub>2</sub></b>	Calcium Carbide
<b>CaO</b>	Calcium Oxide also known as Quicklime/Lime
<b>Cd</b>	Cadmium
<b>Co</b>	Cobalt
<b>Cr</b>	Chromium
<b>Cu</b>	Copper
<b>Cu<sub>2</sub>S</b>	Chalcocite
<b>C<sub>2</sub>H<sub>2</sub></b>	Acetylene
<b>DO</b>	Dissolved Oxygen
<b>DNA</b>	Deoxyribonucleic Acid
<b>Fe</b>	Iron
<b>Fe<sup>2+</sup></b>	Ferrous
<b>FeSO<sub>4</sub></b>	Ferrous Sulphate
<b>Fe<sup>3+</sup></b>	Ferric Iron
<b>FeO</b>	Ferrous Iron
<b>FeS</b>	Pyrrhotite
<b>HCO<sub>3</sub><sup>-</sup></b>	Bicarbonate

<b>Hg</b>	Mercury
<b>H<sub>3</sub>O<sup>+</sup></b>	Hydronium
<b>IARC</b>	The International Agency for Research on Cancer
<b>K-NN</b>	K-Nearest Neighbours
<b>MANFIS</b>	Multi-output Adaptive Neural Fuzzy Inference System
<b>MANFIS-SCM</b>	Multiple Adaptive Neuro-Fuzzy Interference System
<b>MLR</b>	Subtractive Clustering Method
<b>Mn</b>	Multiple Linear Regression
<b>MLP</b>	Manganese
<b>NaOH</b>	Multilayer Perceptron
<b>Na<sub>2</sub>CO<sub>3</sub></b>	Sodium Hydroxide also known as Caustic Soda
<b>Ni</b>	Sodium Carbonate
<b>NN</b>	Nickel
<b>NN-BBO</b>	Neural Network
<b>OH<sup>-</sup></b>	Neural Network
<b>Pb</b>	-Biogeography-Based Optimisation
<b>Radbas</b>	Hydroxides
<b>RMS</b>	Lead
<b>SiO<sub>2</sub></b>	Radial Basis Transfer Function
<b>SO<sub>4</sub><sup>2-</sup></b>	Root Mean Square
<b>(s/s) operations</b>	Silica Sand
<b>SLT</b>	Sulphate/ Sulfate
	Solidification/Stabilization
	Statistical Learning Theory

**SVM-Poly**

Support Vector Machine with  
Polynomial

**SVM-RBF**

Support Vector Machine with radial  
Base Function

**Tansig**

Hyperbolic Tangent Sigmoid Transfer  
Function

**TDS**

Total Dissolved Solids

**Tl**

Thallium

**VLSI**

Very Large Scale  
Integrated Implementability

**Zn**

Zinc

## Glossary

**Acid Mine Drainage (AMD):** Acidic mine water generated during mining activities also Acid Rock Drainage

**Back Propagation Neural Network (BPNN):** A supervised algorithm employed for network training with experimental data-set used to develop the network model.

**Deoxyribonucleic Acid (DNA):** An organic chemical found in most cells of every organism and contains genetic information and instructions for the purpose of protein synthesis.

**Elements:** A substance that is pure which is only made up of atoms with the same numbers of protons in their atomic nuclei.

**General Regression Neural Network (GRNN):** An algorithm based on the estimation of probability density functions and, feature fast training times, and it can model nonlinear functions.

**Heavy Metals:** Chemical metallic elements with relatively high densities, atomic weights, or atomic numbers.

**Learning Algorithms:** The steps used to train networks.

**Light Metals:** Chemical metallic or non-metallic elements with relatively lower densities and atomic numbers.

**Lime:** An inorganic mineral that contains calcium and primarily oxides and hydroxide. The oxides and hydroxides are usually in the form of calcium oxide and/ or calcium hydroxide.

**MATLAB Toolbox:** The MATLAB<sup>®</sup> technical computing environment with a collection of functions built.

**MSE:** A function that tells you how close a regression line is to a set of points.

**Neural Network (NN):** A network of equations where inputs are taken in and outputs returned. Parallel methods of processing information are used and they can extract relationships that are nonlinear and complex.

**Neurons:** Elements where information processing takes place.

**Neutralisation:** An acid and a base react quantitatively with each other in this chemical reaction.

**Neutralising Agents:** An assistant to the qualitative reaction between an acid and a base, known as an emulsifier.

**Precipitation:** Converting the substance into an insoluble form or a super-saturated solution so that the process of converting a chemical substance into a solid from a solution takes place.

**Pyrite (Fool's Gold):** Iron Sulphide ( $\text{FeS}_2$ ) which is considered the most common of the sulphide minerals in ores.

**Reinforcement Learning:** An algorithm with a variation of supervised learning techniques since they continuously analyse the difference between the response produced by the network and the corresponding desired output.

**Solidification/Stabilisation (s/s) Operations:** It is a process that physically encapsulates the contaminants as they are locked in the soil.

**Sulphate/ Sulfate:** A polyatomic anion with  $\text{SO}_4^{2-}$  as an empirical formula.

**Sulphide Bearing Minerals:** A type of ore containing oxygen-free compounds of sulphur found beneath the earth's surface.

**Supervised Learning:** An algorithm where the desired outputs for a given set of input signals are available. It behaves like a “coach”, teaching the network what is the correct response for each sample presented for its input.

**Unsupervised Learning:** An algorithm that does not require any knowledge of the respective desired outputs and where the network organises itself.



## Chapter 1: Introduction

### 1.1 Background of the study

The mining industry in South Africa has managed to elevate the country in the global market and has provided economic benefits over the years. However, these mining activities produce acid mine drainage (AMD) which is acid mine water characterised by a low pH, and high salt and inorganic element (light and heavy metals) contents (McCarthy, 2011). In this dissertation, heavy metals are referred to as chemical metallic elements with relatively high densities, atomic weights, or atomic numbers, while the light metals are referred to as the chemical metallic or non-metallic elements with relatively lower densities and atomic numbers. AMD plays a significant part in contaminating the water system. The cause of interest was brought about by the Cradle of Humankind receiving water that was contaminated by the old gold mines in Krugersdorp. This led to the formation of an investigative committee in late 2010 in order to tackle the arising AMD problems (McCarthy, 2011).

This is a global problem because other parts of the world are also experiencing environmental problems due to AMD. In Southeast Iran, the Sarcheshmeh Mine (where mining of Cu takes place) has played a role in contaminating the Shur River (Rooki et al., 2011). Acidic water is generated during mining when sulphide minerals or pyrite becomes oxidised and the acidic water contains heavy metals, dissolved sulphate ( $\text{SO}_4^{2-}$ ), and iron (Fe) in high concentrations (Rooki et al., 2011).

Oxidation occurs on the pyrite in two stages. The initial stage produces sulphuric acid and ferrous sulphate ( $\text{FeSO}_4$ ) and the second stage produces orange-red ferric hydroxide ( $\text{Fe}(\text{OH})_3$ ) and additional sulphuric acid (McCarthy, 2011). AMD also goes as far as contaminating ground water as in the situation in Arak region. In South Africa and other parts of the world, there is interconnectivity in the groundwater and surface water systems which makes it possible for high volumes of contaminated water to affect the water supply (Ghadimi, 2015).

The heavy metals contained in AMD are of most significant concern because they are non-degradable, therefore making them persist in the environment. They are considered metals with densities that are relatively high, ranging from  $3.5 \text{ gcm}^{-3}$  to  $7 \text{ gcm}^{-3}$ , and are also considered toxic at low concentration levels (Gautam et al., 2014). They are dangerous to the human body, aquatic life, soil and plants.



The bio-accumulative nature in biotic systems is the reason why the hazardous nature of heavy metals was recognised. Mining activities, industrial discharge, and household applications are the carriers of heavy metals into the environment, mostly to nearby water bodies (Gautam et al., 2014).

A study done by Ahsan et al. (2006) stated that arsenic (As) consumed through drinking water led to an increase in the occurrence of skin lesions from a dose as little as 0.0012 mg/kg/day. Lead (Pb) showed toxic effects to the nervous and reproductive systems as well as the kidneys. Bone degradation, renal dysfunction, and blood and liver damage are some of the effects of exposure to cadmium (Cd). High levels of Cu dust exposure cause irritation of the nose, eyes and mouth as well as the possibility of nausea and diarrhea. Even low concentrations of Cu are toxic to a variety of aquatic organisms (Gautam et al., 2014).

Zinc (Zn) is another heavy metal that carries problematic effects. Its toxicity in large amounts causes children to feel nauseated and vomit. It also causes anaemia and cholesterol problems due to a higher concentration of Zn in human beings. Babies who were mentally disturbed and physically deformed were born in Minata Bay (Japan) to mothers who were exposed to toxic mercury (Hg) due to contaminated fish consumption. The major problems of contamination in aquatic systems are also caused by water soluble salts of nickel (Ni) (Gautam et al., 2014). The International Agency for Research on Cancer (IARC), classifies inorganic As and Cd as human carcinogens (International Agency for Research on Cancer, 2014). Cd is a metal and As is a metalloid and both of them are related to the risk of cancer, skin damage and kidney damage as well as other diseases.

Heavy metals also have negative effects on aquatic life. Less than one percent of living mass organisms is contained in heavy metals, and they cause disorders due to their different densities. Oceans receive heavy metals from surface water and acid rain and even though metal pollution of the ocean is low compared to other types of water pollution, these metals affect the marine ecosystem. Fish and other aquatic organisms directly receive the pollutants from water and indirectly through food. Heavy metals have the ability to reduce developmental growth of the aquatic species as well as increase anomalies in development. They can also reduce the chances of survival for the fish at the start of exogenous feeding and even possibly cause fish extinction. Little absorption of manganese (Mn) occurs through the gut via food but high concentrations of it was detected in the gills as the main route of uptake. Higher

concentrations of Fe were found in the livers and lower concentrations in the muscles of fish species (Khayatzaheh & Abbasi, 2010).

There are 13 essential mineral nutrients necessary for a plant's life cycle completion and among them macro-elements are required in large quantities while micro-nutrients are needed in low concentrations (Sela, 2020). Zn and Cu consist of essential micronutrients for the growth of plants, however, at higher levels they may prove to be toxic (Roopali et al., 2017). Some of these plants are the *Argyrodema Testiculare*, the Baby Rubber Plant, the Bunny Ear Cactus, and Aloe Vera, to name a few (Anon., 2013).

Therefore, plants need a certain number of heavy metals to survive. However, once they become toxic, the plant is affected directly and indirectly. Cell structures become damaged by oxidative stress and cytoplasmic enzyme inhibition. These are some of the direct effects of too much heavy metals. The indirect effect is when an essential nutrient in a plant is replaced at cation exchange sites (Chibuike & Obiora, 2014). Indian mustard (*Brassica juncea*) and Water Hyacinths are plants that do not find heavy metals toxic. They can grow in soil that has a high metal concentration and are effective in the extraction of heavy metals such as Pb from the toxic dumping grounds during soil and water treatment (Marry-Lissy & Madhu, 2011).

The general definition of neural networks (NNs) is that they are information processing representations of the biological NN (Rooki et al., 2011). They use a concept of prediction and consist of computing elements or processors, which are models of mathematics with biological neurons interlinked by weights (Vlad, 2004). This concept is presented in this work as a solution for laboratory inconsistencies and was inspired by the biological brain and the nervous system. Although there is a difference between the biological brain and the conventional digital computer. NNs have been applied in many diverse fields over the years and such applications have been found successful and satisfactory. Some of the applications include the recognition of patterns, processing of signals and images, system identification and modelling as well as predictions in the stock market (Sazli, 2006). The reason for such success can be attributed to the fact that NNs are parallel methods of processing information. They are able to extract relationships that are nonlinear and complex (Ghadimi, 2015). Other attributions include the capability to learn and adapt, tolerance of faults, and Very Large Scale Integrated Implementability (VLSI) (Sazli, 2006).

## 1.2 Motivation

The development of any appropriate remediation strategy requires the prediction of the heavy metals in the AMD and this is of great significance. NNs are therefore the tool of such prediction. They are a network of equations that take in inputs and return outputs. They try to mimic brain function which learns through experience. Computers have the challenge of recognising even the simplest of patterns, unlike the brain, which is able to store information as patterns, of which some are complicated. An example is the ability of the brain to allow humans to recognise faces at different angles. A whole new field of computer studies is being investigated where information can be stored as patterns and used to solve problems. This will involve creating parallel networks and training them (Bangal, 2009). NNs are parallel methods of processing information and, they are able to extract relationships that are nonlinear and complex (Ghadimi, 2015).

Plenty of remediation strategies have been developed over the years to treat the AMD after its effect and not before. These treatment processes include hydrated lime or calcium hydroxide ( $\text{Ca(OH)}_2$ ) precipitation which is the conventional process and heavy metal removal processes that are physico-chemical which include adsorption on new adsorbents, electrodialysis, membrane filtration and photocatalysis to name a few (Barakat, 2010).

These treatment processes still require sampling and laboratory analysis for each water source to determine the toxicity (concentrations of heavy metals). This process is time consuming, expensive and may involve human error or negligence. It only gives results for the remediation of already contaminated water. NN is therefore going to bring remediation at a faster rate and solve problems that heavy metals cause to human beings, aquatic life, soil, and plants.

### **1.3 Problem statement**

Acid mine water is characterised by a low pH, high salt and, heavy metal content, and other toxic elements. The heavy metals are non-degradable and are considered metals with densities that are relatively high, ranging from  $3.5 \text{ gcm}^{-3}$  to  $7 \text{ gcm}^{-3}$  and are also considered to be toxic. Some of these heavy metals are Hg, Cd, Pb, antimony (Sb), copper (Cu), Zn, and Fe. These metals are related to the risk of cancer and skin damage as well as kidney damage. Heavy metals also pose a risk for aquatic life (fish), soil, and plants. The conventional method of determining heavy metals present in AMD is time-consuming and expensive due to the fact that it involves taking samples and doing laboratory analysis. AMD prediction is commonly done by laboratory and field tests. The challenge is that AMD formation varies from site-to-site based on a number of different factors. The tests are often done at small scale and during a short period of time which means many uncertainties are introduced for decision-makers when the method is conducted in the large-scale setting of mine sites (Betrie et al., 2012).

This research will investigate using NNs to predict heavy metals in AMD. NNs are parallel methods of processing information and, they are able to extract relationships that are nonlinear and complex. The use of NN will be rapid, reliable, and cost-effective compared to the conventional method of predicting AMD. This will help in eliminating human error that may occur in laboratories. This will allow for the implementation of remediation methods earlier before mining effluents contaminate the environment. This will in turn save river and ground water from being contaminated and reduce or prevent other health risks caused by heavy metals can be reduced if not prevented.

### **1.4. Objective**

To develop a neural network model to predict heavy metals in acid mine drainage from South African mines.

#### **1.4.1 Specific objectives**

- a) To identify AMD and the heavy metals in AMD.
- b) To apply NN.
- c) To find the appropriate algorithm to train the NN.
- d) To compare the NN results (outputs) with the measured concentrations of major heavy metals sampled (targets).

## **1.5 Outline of dissertation**

### **Chapter 1: Introduction**

This chapter provides background information about the study as well as the motivation which reasons and argues why research on this study is necessary. The discussion of the problem statement is done to draw out a connection between the background and motivation. The main and specific objectives of the study are also presented.

### **Chapter 2: Literature Review**

This chapter discusses the literature pertinent to this study. Information about AMD and heavy metals definitions and their sources, AMD chemical formation, and different waste water treatment processes are discussed. The theory of neutralisation and precipitation using different reagents are studied to understand the process of heavy metals removal in waste water. The different NN architectures and algorithms are discussed based on the point of views of different authors, their experiments, and results. The NN architectures and algorithms of importance in this study are discussed and elaborated on further.

### **Chapter 3: Methodology**

The method of carrying out the study gives details of the materials and chemicals that were used. It also explains the procedure of sampling and software training, site identification, description of that site, sample collection, and analysis. The software training procedure gives details on how inputs, targets, and functions were decided upon as well as the steps of training the network using different parameters.

### **Chapter 4: Results and Discussion**

Results obtained are of two samples of raw AMD and neutralised AMD solution. AMD properties were identified in the samples taken from Sibanye Western Basin Treatment Plant. The properties found correspond to the definition of AMD in the literature. Neutralisation using  $\text{Ca(OH)}_2$  proved to be successful in precipitating heavy metals, especially those identified to be problematic. 28 more samples were taken to continue the experiment after finding that the two samples gave lucrative results. The data from the 28 samples were used to train a NN model. The designing of a NN for its application focused on these four important aspects that had to be determined: (1) selection of the backpropagation (BP) training algorithm, (2) data



distribution, where the optimum algorithm was applied to train the NN, (3) selection of the NN structure, and (4) selection of the initial weight.

## **Chapter 5: Conclusion and Recommendations**

This chapter concludes the results and findings of the study and shows how the research addresses the objectives set out for the study. It also gives a way forward on how to continue with the research by giving recommendations on focus areas that could be done differently and could enhance the results of the study.

### **Chapter Summary**

This chapter explains the problems of AMD to the world as a whole as it contaminates other water sources. Heavy metals in high concentrations have been shown to have negative effects on human health, plants, soil, and aquatic animals which motivated the need to treat these water sources. Prior to treatment, laboratory analysis is required to identify and quantify the proportions of light and heavy metals contained in acid mine water samples. This conventional method of determining heavy metals present in AMD is time-consuming, expensive, and may involve human error. The application of NNs is then considered, where NNs are parallel methods of processing information and, able to extract relationships that are nonlinear and complex. The main objective is to develop and train a NN model to predict heavy metals in AMD. The use of NN will be rapid, reliable, and cost-effective compared to the conventional method. This will help in eliminating human error that may occur in laboratories and results will be made available quickly by the predicting model to allow for removal methods to be applied earlier before mining effluents contaminate the environment. The specific objectives of how the project will be carried out are also listed.

## **Chapter 2: Literature Review**

### **2.1 Introduction**

A country's economic wealth and growth largely depends on natural resources. These resources are also important for a country's human-social development (Elçiçek et al., 2014). The mining of coal and gold (natural resources) contributes to the generation of AMD which in turn contributes to the contamination of river and ground water. AMD is formed when the pyrite mineral and oxygenated water come into contact and oxidation of pyrite occurs. In many mineral deposits, pyrite is the minor constituent that is common and is associated with the coal and gold deposits of South Africa. AMD is identified by low pH, high salt content, and most importantly, heavy metals (McCarthy, 2011).

The current impacts of AMD are experienced at both local and regional levels and cause significant deterioration in the quality of scarce water resources. This means that contaminated water puts human health, fish (other aquatic life), and plants at risk (Shah, 2017). This has prompted the world to investigate techniques of predicting heavy metals found in AMD for better ways to manage the contamination and remedy the situation. The technique of interest so far involves the use of NN. NNs are models of mathematics with biological neurons interlinked by weights. These weights are modified during utilisation to satisfy a criterion of performance. The hope is that this technique will be accurate, cost-effective, and rapid (Rooki et al., 2011).

The parameters of this study include learning about NNs and how other researchers have used them to determine how effective, the use of NN is in the prediction process compared to conventional laboratory analysis. There is a need to discover the most effective NN architecture for the best results possible.

### **2.2 Sources and Formation of AMD**

The main source of AMD is mine waste from mines that are either active or abandoned and this AMD is often net acidic (Masindi et al., 2018). Oxidation of sulphide mineral ores is the main cause of AMD. Intensive mining causes them to be exposed to the environment as it contains elevated concentrations of metals and metalloids (Fosso-Kankeu, 2018). Pyrite ore is the most common sulphide mineral and is also known as fool's gold. The combination of water, oxygen, and oxidising bacteria causes the pyrite and sulphide minerals in mine waste to oxidise

and form AMD. Pyrite oxidation is quite complex; therefore, different reactions can represent under different conditions (Kefeni et al., 2017). Some of the examples of reactions for the major and common pyrite oxidation processes are as follows.

The initial reaction involves sulphide mineral oxidation into dissolved Fe,  $SO_4^{2-}$ , and hydrogen which Equation (1) illustrates.



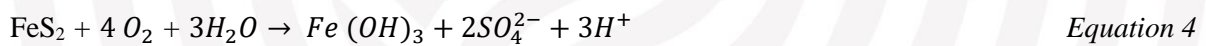
An increase in total dissolved solids (TDS) and acidity in the water is represented by the dissolved Fe,  $SO_4^{2-}$ , and hydrogen. If they are not neutralised, they cause a pH decrease. If the environment contains enough oxygen, pH, and bacteria activity (which are the oxidising requirements), then a lot of the ferrous iron ( $Fe^{2+}$ ) will be oxidised to ferric iron ( $Fe^{3+}$ ), as shown in Equation (2).



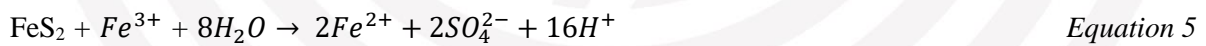
When the pH values lie between 2.3 and 3.5,  $Fe^{3+}$  precipitates as  $Fe(OH)_3$  and jarosite which then leaves a little  $Fe^{3+}$  in the solution while the pH is simultaneously lowered, as shown in Equation (3).



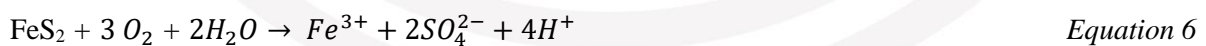
Any  $Fe^{3+}$  from the second Equation that does not precipitate from the solution through Equation 3 can be used to oxidise additional pyrite as shown in Equation (4).



A combination of Equations (1) to (3) represents acid generation that produces Fe which eventually precipitates as  $Fe(OH)_3$ , as shown in Equation 5.



The overall Equation for stable  $Fe^{3+}$  that is used to oxidise additional pyrite is a combination of Equations (1) to (3), as indicated by Equation 6.



All the equations above, except for (2) and (3), have assumed that the mineral being oxidised is pyrite and that oxygen is the oxidant. There are other sulphide minerals like pyrrhotite ( $FeS$ )



and chalcocite ( $\text{Cu}_2\text{S}$ ) which have other ratios of metal sulphide and metals other than Fe. There are different reaction pathways, rates and stoichiometries for additional oxidants and sulphide minerals, however, there is limited research on those variations (Akciil & Koldas, 2005).

The rate of AMD production on a mining site is influenced by many factors such as temperature, bacteria, alternative oxidants (Mn/Fe), and the starting pH. Waste that contains reactive sulphides is considered hazardous materials. Places where these sulphides are found include impoundments, open cuts, pit walls, waste dumps, leach pads, and other areas that are exposed (Kirby, 2014).

Balci and Demirel (2017) worked on predicting the sources that release AMD and metals specifically at the Küre Cu Mine Site, situated in Kastamonu, NW Turkey. There were different methods and criteria used for the classification and assessment of the waste rock's Aquifer Protection Permit (APP) and lithological units around deposits in Küre for the identification of possible sources of AMD generation. Pyrite and chalcopyrite are the most common sulphur minerals that were identified in the wastes. The common gangue minerals were found to be illite, calcite, muscovite, dolomite, feldspar, albite, kaolinite, quartz, olivine, chloride, and gypsum.

The pH value of acid mine water usually ranges around 3, often containing metals such as Fe, Mn, Al, and anions such as  $\text{SO}_4^{2-}$  in high concentrations. Increased concentrations of Zn, Co, Pb, Cr, and Cu have also been observed in acid mine water. It is not always possible to specify typical mine water for individual deposits unambiguously because the source conditions of mine water vary. Incomparable hydrochemical water mixtures can possibly be identified even in one geological structure (Heviánková et al., 2013).

### **2.3 Acid Mine Drainage and Heavy Metals**

AMD is also termed acid rock drainage (ARD) (McCarthy, 2011). It is one of the pollutants in the environment that is caused by mining activities. It is generally characterised by low pH, high heavy metal content and high salinity. Metal concentrations and  $\text{SO}_4^{2-}$  in the water vary based on the properties of the mine. According to Fig (2011), AMD samples were once found to have 5000 mg/L of  $\text{SO}_4^{2-}$  in measure and it was considered to be beyond the maximum point. The toxic and potentially carcinogenic metals found, which were Mn, aluminium (Al), Fe, Ni, Zn, cobalt (Co), Cu, Cd, As, and Pb (Fig, 2011). Elemental silicon was also found but it is chemically inactive and therefore the property that causes lung tissue fibrosis is lacking. However, laboratory animals have been found to experience slight pulmonary lesions due to

intra-tracheal injections of silicon dust. Chronic respiratory effects are likely to be caused by Si (LennTech, 1998-2020).

Over the years, AMD has also been defined as acidic water outflow from mines that are either active or abandoned. Additional risk is posed to the environment because AMD consists of elevated metal concentrations such as Mn, Fe, Al, and other heavy metals and metalloids (Offeddu et al., 2014).

A metalloid is a type of chemical element with properties between those of metals and non-metals or that consists of a mixture of metals and non-metals. There is no standard definition of a metalloid or complete agreement about the elements appropriately classified as metalloids. However, there are six commonly recognised metalloids which are As, Sb, B, Ge, Si, and Te. Al, At, C, Se, and Po are the five elements that are less frequently so classified. A standard periodic table shows all eleven elements located on the p-block in a diagonal region starting from boron on the upper left to astatine on the lower right. In some periodic tables, a dividing line is included between metals and nonmetals with the metalloids being found close to this line (Chemicool, 2017).

The appearance of typical metalloids is metallic; however, they are brittle and only fair conductors of electricity. They have a nonmetal behavior in the chemical state and can form alloys with metals. These metalloids have properties that are intermediate in nature when it comes to their other physical and chemical properties and they are usually too brittle to have any structural uses.

Metalloids can be used in alloys, flame retardants, biological agents, catalysts, optical storage and optoelectronics, glasses, semiconductors, pyrotechnics and electronics (Chemicool, 2017).

Mine drainage can be categorised into two types, net-acidic and net-alkaline. They are both considered highly acidic due to the misconception of the terms acid and acidity. Acid refers to pH while acidity refers to total acidity with both pH and mineral acidity included, meaning that even at a pH of higher than 7, acidity is still possible. The produced concentration of hydrogen ions or hydronium ( $\text{H}_3\text{O}^+$ ) during metal hydroxide ( $\text{OH}^-$ ) formation at a certain pH is referred to as mineral acidity (Moodely et al., 2017).

Lakovleva et al. (2015) highlight that there are three categories of mine water based on the acid-base properties. If the pH is at 6 or below it is considered as AMD. A pH of 6 and above

is considered as neutral mine drainage. A pH greater than 6 which contains carbonates of more than 1000 mg/L, is considered saline mine drainage.

Serious human health and environmental problems may be experienced due to AMD, and this is a global problem (Betrie et al., 2012). The biggest problem with AMD is that it carries with it heavy metals that can cause contamination to soil and, surface and groundwater (Akcil & Koldas, 2005). Such contaminated sources become dangerous to the human body, aquatic life, soil and plants. The heavy metals in AMD are of most significant concern because they are non-degradable, therefore making them persist in the environment. They are considered metals with densities that are relatively high, ranging from  $3.5 \text{ gcm}^{-3}$  to  $7 \text{ gcm}^{-3}$ , and are also considered to be toxic at low concentration levels (Gautam et al., 2014).

According to LennTech (2020), any metallic chemical element with a relatively high density that is toxic at low concentrations is termed a heavy metal. Some of the examples include As, Cd, Cr, Hg, Tl, and Pb. They are the natural components found in the Earth's crust, which cannot be degraded or destroyed. Food, air and drinking water are some of the ways in which these metals enter our bodies to a small extent. The human body needs some heavy metals in the form of trace metals, such as Cu, Zn, and Se, as they are essential to maintain the body's metabolism. Poisoning only occurs if these metals are in higher concentrations as a result of drinking water from lead pipes, breathing in high ambient air concentrations near emission sources or food intake.

Metals that also pose health risks include antimony (Sb) which can cause heart diseases and cholesterol, Pb which can be linked to anaemia, Hg which can be linked to kidney and liver damage, and gastrointestinal disorders which can be attributed to Cu (Malik & Khan, 2016). Even if the level of exposure to these metallic elements (Hg, As, and Pb) is low, they have the ability to induce toxicity (Jan et al., 2015).

The heavy metals of most concern are As, Cd, Ni, Cr, Cu, Hg, and Pb, because they have negative effects on human health and are found in high concentrations in drinking water in some areas. In one's lifetime, drinking 1 L/day of water contaminated with  $50 \mu\text{g/L}$  of As could potentially lead to liver, kidney, bladder, and lung cancer in 13 out of 1000 people (Smith, Lingas and Rahman, 2000). However, as stated by Moodley et al. (2017), the  $\text{SO}_4^{2-}$  and metal concentrations in the acid water vary based on the mine characteristics and therefore other metals can be of concern to living organisms and the environment.

Jan et al. (2015) detail the dangers that heavy metals pose to the human body. The human body has control mechanisms which metals can escape and cause lethal effects on the body. Some of the control mechanisms include transportation, homeostasis, specified cell constituents binding and compartmentalisation. The ability of heavy metals to displace metals of importance from their sites can lead to cellular process malfunction in the body.

The primary cause of oxidative deterioration of the biological macro-molecules is the binding of metals to the deoxyribonucleic acid (DNA) and nuclear proteins. Contamination can be seen through symptoms which may include disorders of the central nervous system, insomnia, depression, intellectual disability in children, kidney and liver diseases and instability of emotions. Basically, if the exposure to toxic metals (symptoms) is not identified and treated properly, an important medical problem can be experienced which will lead to an increase in the rate of morbidity and mortality (Jan et al., 2015).

Aquatic animals such as fish experience situations where heavy metals gather in their various organs which then leads to death. The effects of the heavy metals are first observed in the blood of the fish where its blood components are altered and it becomes weak, anaemic, and left exposed to diseases. The haematological indices of the fish are increased or decreased which leads to a decline in the protein and glycogen reserves due to heavy metals (Shah, 2017). Heavy metals can reduce developmental growth of aquatic species as well as increase anomalies in developments. They can also reduce the chances of survival for the fish at the start of exogenous feeding and even possibly lead to fish extinction. Little absorption of Mn occurs through the gut via food but high concentrations of it was detected in the gills as the main route of uptake. Higher concentrations of Fe were found in the livers and lower concentrations in the muscles of fish species (Khayatadeh & Abbasi, 2010).

Heavy metals affect the soil and plants which grow from it. Metals can either combine with soil components or exist separately. The components that metals may exist with could be exchangeable or nonexchangeable ions, or insoluble inorganic metal compound such as carbonates and silicate minerals. Metals that exist separately are the ones that cause pollution while those that attach themselves to silicate minerals do not cause any contamination and simply represent the background soil metal concentration. The heavy metals which are available as soluble components in soil solutions are the ones that are required for the plant uptake (Chibuike & Obiora, 2014).

There 13 essential mineral nutrients necessary for a plant's life cycle completion and it requires macro-elements in large quantities and micro-nutrients in low concentrations (Sela, 2020). Zn and Cu consist of essential micronutrients for the growth of plants, however, at higher levels they may prove to be toxic (Roopali et al., 2017). Some of these plants are the *Argyrodema Testiculare*, the Baby Rubber Plant, the Bunny Ear Cactus, and Aloe Vera, to name a few (Anon., 2013). Heavy metals contribute negatively to the activities and growth of micro-organisms in the soil, and this could affect the growth of plants indirectly. When heavy metals cause a reduction in beneficial soil micro-organisms, it could lead to a reduction in the decomposition of organic matter and ultimately reduce the soil nutrients. When heavy metals interfere with soil microorganisms, they tamper with enzyme activities which are necessary for plant metabolism. All the above-mentioned direct and indirect toxic effects of heavy metals can inhibit the growth of the plant or even kill it (Chibuike & Obiora, 2014).

Therefore, plants need a certain number of heavy metals to survive. However, once they become toxic, the plant is affected directly and indirectly. Some of the direct effects of too much heavy metals include cell structures becoming damaged by oxidative stress and cytoplasmic enzyme inhibition. The indirect effect is when an essential nutrient in a plant is replaced at cation exchange sites (Chibuike & Obiora, 2014). Indian mustard (*Brassica juncea*) and Water Hyacinths are plants that do not find heavy metals toxic. They can grow in soil that has a high metal concentration and are effective in the extraction of heavy metals such as Pb from toxic dumping grounds during soil and water treatment (Marry-Lissy & Madhu, 2011).

## **2.4 AMD Treatment Methods**

There is a wide variety of treatment options with the ability to accomplish the task of remedying industrial wastewater of heavy metals. A few of them include chemical precipitation, solvent extraction, activated carbon adsorption, foam flotation, complexation, electro-deposition, coagulation, cementation, ion exchange and membrane operations. The most common treatment options are chemical precipitations (because it is most economical), ion exchange, conventional adsorption, electro-remediation methods, and membrane separation methods (Gunatilake, 2015).

The most important step in acid mine water treatment is acid neutralisation or neutralisation of acid water. Effective treatment methods are used for the purpose of neutralising pH and, removing harmful ions and suspended solids. After treatment, mine water quality must result in water quality indicators that are able to sustain life conditions for organisms in rivers and



can be utilised for further uses of water such as service water. The neutralisation of mine water using various agents has been studied, world-wide in numerous localities with the occurrence of acid mine water. Some of these agents are  $\text{Ca}(\text{OH})_2$  or portlandite (also known as calcium oxide ( $\text{CaO}$ ) or slacked lime or quicklime mixed with water), calcium carbonate (also known as limestone ( $\text{CaCO}_3$ )),  $\text{CaO}$  and caustic soda ( $\text{NaOH}$ ) (Heviánková et al., 2013).

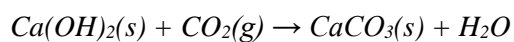
$\text{CaO}$  is a white crystalline solid and its melting point is  $2572^\circ\text{C}$ . The manufacturing of  $\text{CaO}$  involves heating  $\text{CaCO}_3$  items such as limestone, sea-shells, coral, or chalk to drive off carbon dioxide ( $\text{CO}_2$ ), as Equation (7) illustrates.



This is a reversible reaction where  $\text{CaO}$  can react with carbon dioxide to form  $\text{CaCO}_3$  again. In order to drive this reaction to the right,  $\text{CO}_2$  is flushed from the mixture as it is released. This reaction is one of the oldest chemical transformations produced by man with its use predating recorded history. The word  $\text{CaO}$  is found in most ancient languages such as Latin, where it is known *calx*. *Calx* is the word from which the calcium element got its name. The name of this element in old English is *lim*, which serves as the origin of the commercial name known as lime (Science is fun in the laboratory of Shakhashira, 2017). It has so many uses but the oldest uses of lime have focused on the regeneration of  $\text{CaCO}_3$  by exploiting its ability to react with carbon dioxide. A mixture of lime with sand and water results in mortar, which has long been used in securing bricks and stones together in construction. When laid in bricks, mortar starts off as a stiff paste that hardens gradually to cement those bricks together (Science is fun in the laboratory of Shakhashira, 2017).

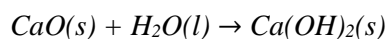
According to Cavalcante et al. (2010)  $\text{Ca}(\text{OH})_2$  is described by Estrela et al. (1994) as an alkaline powder (white in colour) with poor solubility in water. It has a pH of 12.8, which makes it a strong base which can be formed by reversing a  $\text{CaCO}_3$  reaction or calcining or roasting  $\text{CaCO}_3$  until it transforms into  $\text{CaO}$ .  $\text{CaO}$  can be hydrated to form  $\text{Ca}(\text{OH})_2$  and the reaction between the latter and  $\text{CO}_2$  leads to  $\text{CaCO}_3$  formation. Equations (8), (9), and (10) represent these reactions.



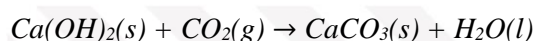


*Equation 10*

CaO reacting with CO<sub>2</sub> at room temperature is a very slow process, however, the addition of water speeds it up. Therefore, to reduce the hardening time of mortar, CaO is mixed with water to form Ca(OH)<sub>2</sub> so that when it reacts with CO<sub>2</sub>, the reaction to form CaCO<sub>3</sub> is faster. This is shown in Equations (11) and (12).



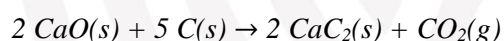
*Equation 11*



*Equation 12*

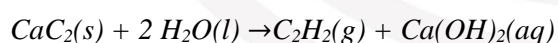
Portland cement and CaO plaster form part of more quicklime based products in the construction industry. Glass production from quicklime is one of the oldest reactions using CaO. The heating of CaO with silica or sand (SiO<sub>2</sub>) and sodium carbonate (Na<sub>2</sub>CO<sub>3</sub>) forms a solution that hardens into an amorphous (non-crystalline) phase, clear and colourless solid instead of crystallising when it is cooled. Glass does not have a distinct melting point because it is a mixture, so it softens gradually as it is heated. This is the result of one of the important qualities of quicklime the ability to form solutions with silicates (Science is fun in the laboratory of Shakhshira, 2017).

Quicklime has played an important role in chemical manufacturing where it is used to produce calcium carbide (CaC<sub>2</sub>), which is manufactured by heating CaO with coke. See Equation (13).



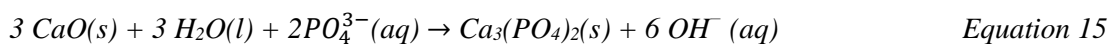
*Equation 13*

Reacting CaC<sub>2</sub> with water yields acetylene (C<sub>2</sub>H<sub>2</sub>), which plays a vital role as a welding fuel and as a starting material for raw materials of polymers, as shown in Equation (14).

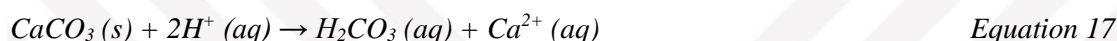
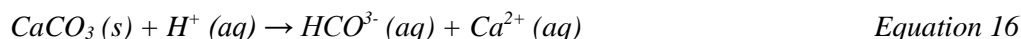


*Equation 14*

Another important use for quicklime is its addition to sewage for phosphate removal. See Equation 15.



Water supply pretreatment makes use of lime to decrease the acidity, soften and clear drinking water (Science is fun in the laboratory of Shakhshira, 2017).  $\text{CaCO}_3$  is an agent found in rocks such as limestone and through the following reactions, it can neutralise the acid.  $\text{CaCO}_3$  has in fact been used in treating AMD water in treatment plants as well. See Equations (16) and (17).



The pathways of both reaction Equations (16) and (17) indicate the acid ( $\text{H}^+(aq)$ ) as a reactant and is therefore consumed. The  $\text{H}^+(aq)$  decrease will lead to acidity decrease while the pH increases (Garland, 2011). pH changes steadily over the pH range as acidic water/waste water/AMD is neutralised by an alkaline by any of the agents mentioned above. The pH is bound to end up on the alkaline side when excess alkali is added. Different neutralising agents have different effects, with CaO expected to take the pH across to a moderately alkaline value of about 10 or lower while limestone should take the pH change only as far as about 7, depending on the acidic water/waste water/AMD complexity (Nuttfield, 2020). Mine Wastewater Treatment Plant (MWTP) Svatava focuses on the elimination of high Fe contents, lowering the concentration of Mn and suspended solids, and controlling of mine water with low pH values (Heviánková et al., 2013).

Caustic soda, also known as sodium hydroxide, is produced naturally as a co-product during chlorine production, which is electrolysis of sodium chloride. According to the laws of chemistry, for every tonne of chlorine, 1100 kg of caustic soda and 28 kg of hydrogen can be produced. Most of the time it is traded as an aqueous solution, but it can also be traded as concentrated solid pellets, flaks, or bulk fused. The important properties of caustic soda are that it is a strong hydrophilic and highly alkaline, which makes it highly corrosive to skin tissue. It is hazardous to plants and animals and therefore, it is important to avoid unprotected direct physical contact. It is not volatile (EuroChlor, 2016).

### **Neutralisation and precipitation**



Chemical precipitation involves the addition of chemicals to transform a soluble compound into an insoluble form. A fine line exists between chemical precipitation and solidification/stabilisation (s/s) operations. The contaminants are rendered less prone to leaching in s/s operations, because they become incorporated into a cement-like matrix. The objective of s/s technologies is to ensure that the leaching potential of the contaminants is minimised. This is no different from chemical precipitation where the objective is to make the contaminant less soluble (Peters & Shem, 1998).

Solidification/stabilisation operations techniques immobilise heavy metals as well as organic contaminants because organics with low water solubility are generally immobilised fairly well in this technique, unlike those with high solubility. The difference between the two techniques is visible in that it is rare for precipitation to be used on organic compounds, although organics can adsorb or absorb onto precipitate forms such as hydrous metal oxides (Peters & Shem, 1998).

Metal-containing wastewater is commonly treated by the chemical precipitation technique with oxidation/reduction plus precipitation as a closely related technique. Precipitation has its own advantage, namely a high volume can be treated at a low cost. High ionic strength often improves the process and it is a reliable process which is well suited for osmotic control. However, its disadvantages include stoichiometric chemical addition requirements, the disposal of high-water-content sludge, flows are small and intermittent which makes them not ready for processing ready and application, and two-stage precipitation may be required for a part per billion effluent contaminant. There are three stages through which precipitation proceeds: nucleation, crystal growth, and flocculation. Hydroxide precipitation (primarily hydroxide treatment) is usually employed to accomplish treatment of wastewater. Precipitation treatment is employed by nearly 75% of plating facilities as the treatment technique scheme for heavy metals removal from solutions (Peters & Shem, 1998).

The treatment of AMD has been using six primary chemicals and each one is more or less appropriate for a specific condition based on its characteristics. Technical factors (levels of acidity, flow, the metal types and concentrations in the water, the required rate and degree of chemical treatment, and the final water quality desired) and economic factors (reagent prices, labour, machinery and equipment, the number of years that treatment will be needed, the interest rate, and risk factors) determine the best choice among the different alternatives (Lehigh Earth Observatory EnviroSci, 2011).

For the dissolved metals in water to form insoluble metal hydroxides and settle out of the water, enough alkalinity must be added for the water pH to be raised and  $\text{OH}^-$  to be supplied. The pH range of 6 to 9 is required for most metals to precipitate from water, except for  $\text{Fe}_2\text{O}_3$ , which precipitates at a pH of about 3.5. Therefore, the types of metals as well as their amounts in the water have a great influence when it comes to selecting an AMD treatment system. At a pH greater than 8.5, FeO is converted to a solid bluish-green ferrous hydroxide ( $\text{Fe}(\text{OH})_2$ ). As expected when oxygen is present,  $\text{Fe}^{2+}$  is oxidised to  $\text{Fe}^{3+}$  while  $\text{Fe}(\text{OH})_3$  forms a yellowish-orange solid known as yellow boy, which precipitates at a pH greater than 3.5 (Lehigh Earth Observatory EnviroSci, 2011).

In AMD without oxygen exposure, Fe is primarily in the  $\text{Fe}^{2+}$  state and this means that enough alkalinity must be added to raise the pH of the solution to 8.5 before  $\text{Fe}(\text{OH})_2$  precipitation occurs. The efficient treatment of high  $\text{Fe}^{2+}$  AMD requires that the AMD be initially outgassed of the  $\text{CO}_2$ , also known as aeration of water. This causes the  $\text{Fe}^{2+}$  to convert to  $\text{Fe}^{3+}$  so that the addition of a neutralising chemical raises the pH to 6 or 7 and  $\text{Fe}(\text{OH})_3$  is formed. There is also a benefit to aeration post-chemical addition because it reduces the amount of neutralising reagent required to precipitate Fe from AMD (Lehigh Earth Observatory EnviroSci, 2011).

The general precipitation pH of aluminium hydroxide ( $\text{Al}(\text{OH})_3$ ) is at  $\text{pH} > 5.0$ . However, it also redissolves into a solution to form aluminate ( $\text{AlO}_2^-$  or  $\text{AlO}_3^{-3}$ ) at a pH of 9.0. Mn precipitation varies based on its many oxidation states. However, the general pH of Mn precipitation is at a pH of 9.0 to 9.5. A pH of 10.5 is sometimes necessary for the complete removal of Mn. As much as the oxidation state and concentrations of metals determine the appropriate treatment chemical, another factor to take into consideration is that the interactions among metals have an influence on the degree and rate of precipitation. For instance, if Fe concentration in the water is about four times greater than the Mn content, Fe precipitation is largely able to remove Mn from the water at a pH of 8 due to co-precipitation. Co-precipitation may not remove Mn if the Fe concentration in the AMD is not greater than the Mn content because a pH greater than 9 is required to remove Mn (Lehigh Earth Observatory EnviroSci, 2011).

AMD consists of various combinations of acidity and metals, making each AMD unique. This means that different sites will require unique treatment by the appropriate chemicals. It is possible that AMD from one site, at pH 8.0 is completely neutralised and contains no dissolved

solids but another site may still have metal concentrations that fail to meet effluent limits even after the pH has been raised to 10 (Lehigh Earth Observatory EnviroSci, 2011).

When caustic soda is used to adjust the pH of a solution to convert dissolved (ionic) metals into insoluble particles, metal hydroxides form as expected. There are several conditions that affect the results that are obtained, and one is the pH of the solution. Every metal within an AMD sample has a specific pH at which optimum hydroxide precipitation can take place. Take Cd, for instance, which can achieve optimum precipitation at a pH of 11.0. Other examples include Cu at pH 8.1, Cr at pH 7.5, Ni at pH 10.8 and Zn at pH 10.1. Metal hydroxides are of amphoteric nature (increased solubility at both low and high pH). The point of minimum solubility is achieved at different pH values for every metal. The solubility of one metal hydroxide may be minimised at a certain pH while another metal hydroxide's solubility is relatively high at that very same pH. Therefore, a slight change in pH causes  $\text{OH}^-$  to start going back into the solution since metal hydroxides are quite soluble (Water Specialists Technologies, 2020).

## **2.5 Application of Neural Network**

NNs have been applied in many diverse fields over the years and such applications have been found successful and satisfactory. Some of the applications include the recognition of patterns, processing of signals and images, system identification and modelling, and predictions in the stock market (Sazli, 2006). The reason for such success can be attributed to the fact that NNs are parallel methods of processing information and that they are able to extract relationships that are nonlinear and complex (Ghadimi, 2015). Other attributions include the capability to learn and adapt, tolerance of faults and Very Large Scale Integrated Implementability (VLSI) (Sazli, 2006).

The inspiration of NNs came from their biological counterparts (the biological brain and the nervous system). However, there is a difference between the biological brain and the conventional digital computer based on its structure and the manner of information processing. The biological brain can “learn” and “adapt” but a conventional computer can only accomplish specific tasks by following instructions loaded onto it, which are known as “programmes” or “software” (Sazli, 2006).

A NN consists of computing elements or processors, which are models of mathematics with biological neurons interlinked by weights. These weights are modified during utilisation to

satisfy a criterion of performance. A NN basically adds up the signal that comes from its inputs and multiplies them with the correspondent weights. If the result goes beyond the threshold, the neuron can fire and transmit a signal at the output using a transfer function (Vlad, 2004).

Rooki et al. (2011) used four main assumptions to explain the mechanism of NNs. The first one indicated that the processing of information happens in neurons which are simple processing elements. The second stated that information signals travel between the neurons through connection links. The third stated that the signal that is being transmitted is multiplied at the connection link due to the weight it is associated with. The fourth indicated that an activation function is applied on the net input by the neuron to get an output signal.

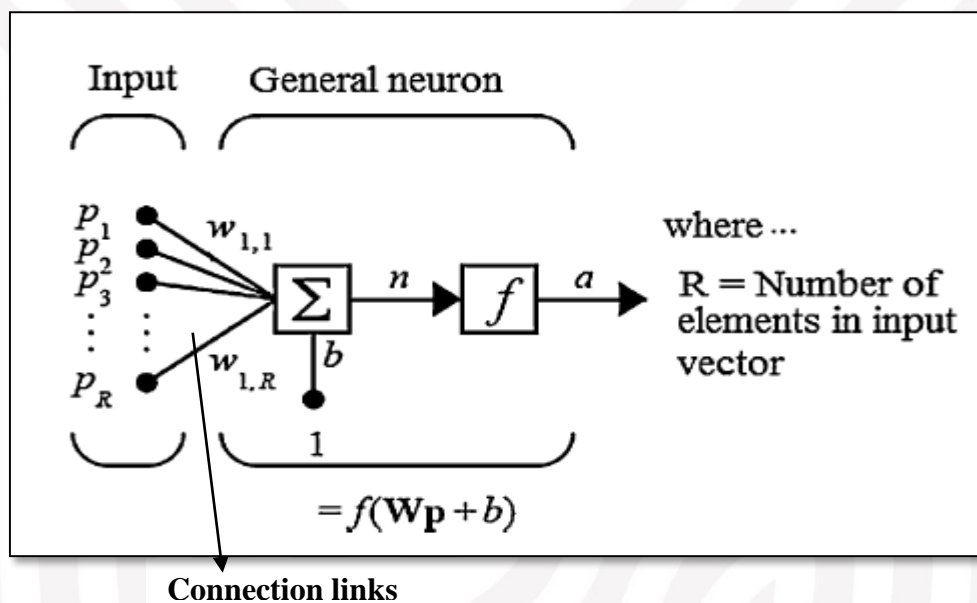


Figure 1: Image of a typical neuron (Rooki et al., 2011)

NNs, like every other thing, have their own advantages and disadvantages. A NN is not a tool that is universal for problem-solving, so there is no existing method to choose, train, and verify a suitable NN. The NN requires excessive training time based on the data set accuracy and quality. It is able to learn an input data set as well as the output responses very well, but its abilities of generalisation may be poor. It can work well with a data-set that is missing and incomplete (Vlad, 2004).

The selection of appropriate architecture and the network training choice are crucial steps (Rooki et al., 2011). NNs can be categorised into two main network architectures: feed-forward NNs and recurrent NNs. This is based on the way in which the neurons are connected. A NN

is referred to as feed-forward if there is no feedback from the outputs of the neurons towards the inputs throughout the network. However, if such a connection exists, which is known as a synaptic connection, then it is called a recurrent NN. This also applies if the feedback connection is towards their own inputs or the inputs of other neurons. NNs are arranged in layer form. Feed-forward and recurrent NNs can also be categorised based on the number of layers which are either single layer or multi-layer (Sazli, 2006).

A single-layer structure consists of two layers (the input and output layer) with the input not counted because no computation takes place in that layer. On the other hand, a multi-layer structure consists of at least one or more hidden layers which are useful for intervening between the external input and the network output between the input and output layer. Higher-order statistics can be extracted by the network because of the hidden layer. The NN structure is named based on the number of neurons in each layer. If there is a connection between every neuron in each layer to every neuron in the next layer, the network is considered fully connected, but if some connections are not there, then the network is considered partially connected (Sazli, 2006).

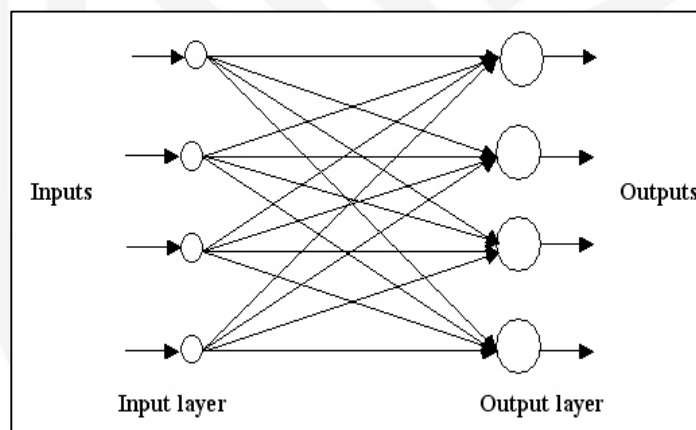


Figure 2: A single-layer feed-forward NN (Sazli, 2006)



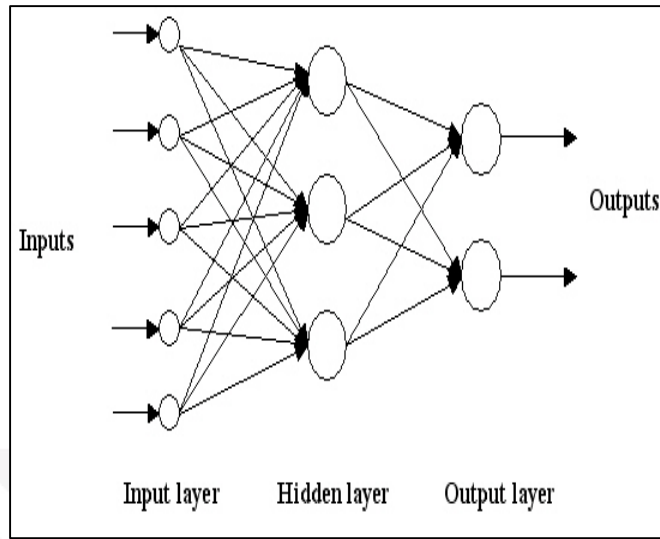


Figure 3: A multi-layer feed-forward NN (Sazli, 2006)

In order for the NN to perform all the tasks that have been observed, a process of learning, known as a learning algorithm, has to take place. This is a process where a NN learns from its environment and improves its performance. Learning is defined as a process of using environmental stimulation in which the network is embedded to adapt free parameters of a NN. There are different types of learning, and they are determined by the way in which the parameter changes occur (Sazli, 2006).

Different architectures and algorithms to predict various contaminants in ground water and AMD using a variety of methods have been studied and some of the results obtained from those methods are discussed to understand which method has worked best so far. Rooki et al. (2011) used a NN in Southeast Iran for heavy metal prediction in AMD. The Shur River was used as the site of sample collection since it received AMD from the Sarcheshmeh Porphyry Cu Mine.

Three algorithms were considered and compared: the Backpropagation Neural Network (BPNN), the General Regression Neural Network (GRNN), and the Multiple Linear Regression (MLR). The correlation coefficients values were high between the heavy metals and concentrations of pH,  $SO_4^{2-}$ , and  $Mg^{2+}$ , which is why these concentrations were chosen as input data for the NN models (Rooki et al., 2011).

The BPNN was multi-layer (three layers) with a *tansig* activation function applied in the hidden layer and a linear activation function on the output layer. The GRNN was also multi-layer

(three layers) with a *radbas* activation function applied in the hidden layer and a linear activation function on the output layer. The correlation coefficient (R) and root mean square (RMS) were used to compare the effectiveness of the three NNs for training and test data (Rooki et al., 2011).

The authors found that between the predicted concentrations and data measured, a close agreement was observed when the BPNN and GRNN were used. The MLR resulted in low prediction capability because low correlation values were observed between the predictions of the model and the data measured. They then concluded that the BPNN and GRNN algorithms were more effective in predicting heavy metals in AMD compared to the MLR (Rooki et al., 2011).

It is crucial to note that the automated Bayesian regularisation was implemented for the training of the BPNN. Two subsets of data were developed. One subset was the training set for the purpose of computing the gradient and updating the network weights and biases. The other subset was the test set. This is where the mean square error (MSE) method was used. It modified the performance function chosen to be the sum of squares of the network errors on the training set. Feed forward NNs are trained using the typical performance function known as the mean sum of squares of the network errors illustrated in Equation (18).

$$MSE = \frac{\sum (SP_{cal} - SP_{exp})^2}{N} \quad \text{Equation 18}$$

There are plenty of other performance functions used to assess the effectiveness of NNs. The simple linear regression is one of them and it used the least squares method to find the line of best fit for a set of paired data, also known as the best linear equations (BLE). The line of best fit is described by Equation (19).

$$\hat{y} = bX + a \quad \text{Equation 19}$$

This equation allows for the estimation of the value of a dependent variable (Y) from a given independent variable (X). *b* defines the slope of the line and *a* is the intercept.

Machine learning techniques were studied for the development of models that would be used to predict the quality of AMD. The mine site's historical data was used. The following machine learning techniques were considered: NN, support vector machine with radial base function (SVM-RBF) kernels, support vector machine with polynomial (SVM-Poly), K-nearest neighbours (K-NN), and model tree (M5P). The identification of physico-chemical parameters

(which are referred to as input variables) with the ability to influence drainage dynamics was done. This was then used for the development of models that would predict concentrations of Cu. The evaluation of uncertainty and predictive accuracy of the chosen techniques was reliant on various statistical measures. The SVM-Poly proved to be the best performing technique, followed by the SVM-RBF, NN, M5P, and K-NN. These results led to the conclusion that there is great potential for machine learning techniques as tools for AMD quality prediction (Betrie et al., 2012).

Gholami et al. (2011) compared the support vector machine and BPNN techniques. The SVM is a novel method of machine learning which is based on statistical learning theory (SLT). One of the features is that the problem of kernel and the nature of the optimisation requirement leads to a uniquely global optimum, high performance of generalisation, and local optimal solution converging prevention. The authors showed a comparison of the application of SVM and BPNN to predict Fe and Ni concentrations using the chemical and physical parameters found through a sampling process conducted in the Sarcheshmeh Cu mine in Iran. The methods are both data-driven, however, SVM results in higher accuracy and a faster running time. Less RMS error was observed with the SVM. Running time is an important factor when choosing a model that is appropriate and high-performing data-driven. A smaller fraction of computational time is required by SVM than with the BPNN (Gholami et al., 2011).

The development of proper remediation strategies for ground water contamination is dependent upon the ability to predict heavy metals. The study done by Ghadimi (2015) was to attempt to predict Pb, Cu and Zn in the Arak City groundwater by using a NN algorithm. These heavy metals are associated with bicarbonate ( $\text{HCO}_3^-$ ) and  $\text{SO}_4^{2-}$  to form heavy metal  $\text{HCO}_3$  and  $\text{SO}_4^{2-}$  species in water. There was high Pb, Zn, and Cu concentrations found, which were emitted by sources that were anthropogenic. The proposed NN model was generated using a dataset which consisted of 150 samples. The input parameters used were  $\text{HCO}_3$  and  $\text{SO}_4$  while the output parameters were the heavy metals (Pb, Zn, and Cu). The conclusion was made that the reliable system modelling technique for heavy metal estimation in Arak City groundwater is NN, and it did so with a high degree of accuracy and robustness. The Multilayer Perceptron (MLP) NNs model method showed low capability of predicting heavy metal concentrations due to the low correlation values between the predictions of the model and the measured data (Ghadimi, 2015).



Sadeghiamirshahidi et al. (2013) applied the NN model to predict the oxidation of pyrite in the spoil of the Alborz Sharghi coal washing refuse pile located in Northeast Iran. The input parameters for the network included the spoil depth, initial pyrite amount that the spoil particle contained, annual precipitation, and the effective diffusion coefficient. The amount of pyrite remaining in the spoils at various depths counted as the output of the network.

Sadeghiamirshahidi et al. (2013) applied the feedforward network which is the simplest network and entails data moving in one direction. Data moved through the input nodes and left through the output nodes. The neurons have weights and biases that are learnable. It was applied with the back-propagation learning algorithm with an arrangement of 4-7-4-1 which was found to have the capability of predicting the pyrite oxidation rate. Three trenches over the refuse pile were considered and the network predicted the remaining pyrite at various depths. There was a very close similarity between the values obtained by the network during simulation and the experimental results.

Fard et al. (2017) contributed by using NN to determine heavy metal distribution in groundwater so that necessary strategies of management could be developed at mining sites. The authors of this paper explored artificial intelligence in varieties wide than just NN. NN, the multi-output adaptive neural fuzzy inference system (MANFIS) and hybrid NN with biogeography-based optimisation (NN-BBO) were considered to estimate heavy metal distribution in the Lakan Pb-Zn mine's groundwater. The groundwater quality monitoring data that already existed were used to determine groundwater contaminants. The collected data was used to train and test several models to find the optimum model which used three inputs and four outputs. The MANFIS model was found to have the best chances of estimating heavy metal distribution in groundwater when the predicted and measured data were compared. It was found to have a high degree of robustness and accuracy (Fard et al., 2017).

Fard et al. (2017) were able to determine high concentrations of Fe, Mn, Pb and Zn in the groundwater of the Lakan Pb-Zn mine as output parameters. This was attributed to historical mining operations. The input parameters used for NN, NN-BBO, and MANFIS-SCM models were  $SO_4^{2-}$ , Cl, and TDS. They concluded that it demonstrated in detail the implementation of a hybrid for BBO as an optimiser of connecting weights of NN for the prediction of heavy metal concentrations in groundwater. They also made clear that the MANFIS-SCM model was the best option to estimate heavy metal concentrations in groundwater due to its accuracy.

One of the most significant processes for industries that produce boric acid or fabricate heat resistant glass and cleaning agents is dissolution. An examination was done on the dissolution of colemanite water saturated with carbon dioxide solutions. NN, the type based on MLP, was used to predict the dissolution rate. The input parameters for the network were reaction temperature, stirring speed, total pressure, particle size, reaction time, and solid/liquid ratio. The MLP was trained by an experimental dataset so that dissolution kinetics could be predicted. The predictions were considered highly accurate compared to those obtained from the regression model. They therefore concluded that conventional statistic methods for prediction of boron minerals are not as accurate and the best alternative would be to use NN (Elçiçek et al., 2014).

Stream water quality has been tested using dissolved oxygen (DO) as a primary indicator. Ways to retain stream water quality and DO concentration maintenance using different pollution control activities have been a big social problem. The use of NN has assisted in the estimation of DO concentrations, downstream of Mathura City in India, located at the bank of the Yamuna River in the state of Uttar Pradesh (Sarkar & Pandey, 2015).

The most commonly used technique is the feedforward error back propagation NN. Mathura (upstream), Mathura (central), and Mathura (downstream) are the three locations that were considered with the following parameters being used for analysis: monthly data sets on temperature, biochemical oxygen demand (BOD), flow discharge, pH and DO. Three types of NN models were developed using NN with the use of different input variables combined and input stations. The input variables were (a) all the data sets for stations Mathura (upstream, central, and downstream), except the DO values at Mathura (downstream), (b) all data sets for the stations Mathura (upstream and central), and (c) all the data sets for the stations Mathura (upstream). Statistical tools used to evaluate the NN technique performance were coefficient of correlation and RMS. The predicted DO values with high correlations between the values predicted and measured showed prominent accuracy (Sarkar & Pandey, 2015).

Table 1: Summary of some research done on NN technology by different authors

Topic	NN Used	Reference
Prediction of heavy metal concentrations in AMD using neural networks from the Shur River of the Sarcheshmeh Porphyry Cu Mine, Southeast Iran.	Backpropagation Neural Network, General Regression Neural Network, Multiple Linear Regression	(Rooki et al., 2011)
Predicting Cu concentrations in AMD: a comparative analysis of five machine learning techniques.	Neural Networks Support Vector Machine with Radial Base Function (SVM-RBF) Kernels Support Vector Machine with Polynomial (SVM-Poly) K-Nearest Neighbours (K-NN) Model Tree (M5P).	(Betrie et al., 2012)
Prediction of toxic metal concentrations using artificial intelligence techniques.	Support Vector Machine Backpropagation Neural Network	(Gholami et al., 2011)
Prediction of heavy metal contaminations in the groundwater of the Arak region using neural networks and multiple linear regression.	Neural Network Multilayer Perceptron Neural Networks Model	(Ghadimi, 2015)
Applied neural network model to predict the oxidation of pyrite in the spoil of the Alborz Sharghi coal washing refuse pile located in Northeast Iran.	Feed-Forward Network Back-propagation Learning Algorithm	(Sadeghiamirshahidi et al., 2013)
NN to determine heavy metal distribution in groundwater so that	Multi-output Adaptive Neural Fuzzy Inference System (MANFIS)	(Fard et al., 2017)

<p>necessary strategies of management could be developed at mining sites.</p> <p>Examination was done on the dissolution of colemanite water saturated with carbon dioxide solutions</p>	<p>Hybrid NN with Biogeography-Based Optimization (NN-BBO)</p> <p>Multilayer Perceptron (MLP)</p>	<p>(Elçiçek et al., 2014)</p>
<p>The use of NN in the estimation of DO concentrations, in stream water, downstream of Mathura City in India, located at the bank of the Yamuna River in the state of Uttar Pradesh</p>	<p>Backpropagation Neural Network (BPNN)</p>	<p>(Sarkar &amp; Pandey, 2015)</p>

## Chapter Summary

This chapter explained in detail the definition of AMD and heavy metals. The source of AMD, which is pyrite and other sulphide minerals, as well as its chemical species formation in wastewater were also discussed. Wastewater is treated in different ways, and the special method used to treat AMD to prevent contamination of pure water sources investigated. The theory of neutralisation and precipitation using different reagents was studied in order to understand the process of heavy metals removal in waste water. NNs can ensure that water treatments and other remediation treatments are applied quicker without going through laboratory delays. The different NN architectures and algorithms were discussed based on different authors' point of view, experiments, and results to assist in the methods that will be used in this project to predict heavy metal concentrations in water.

## Chapter 3: Methodology

### 3.1 Materials and Chemicals

Samples of raw AMD (30) and neutralised AMD (8) from Sibanye Western Basin AMD Plant in Randfontein, which collects AMD from Shaft 9 in the western area, were collected using 2L sample containers. 10%  $\text{Ca}(\text{OH})_2$  was used as the neutralising agent for raw AMD. The dosing was done according to the pH. A lower pH required more lime to be dosed. A pH probe was used to send the information to the programmable logic controller (PLC) which controls the speed of the pump supplying the lime.

### 3.2. Experimental Procedure

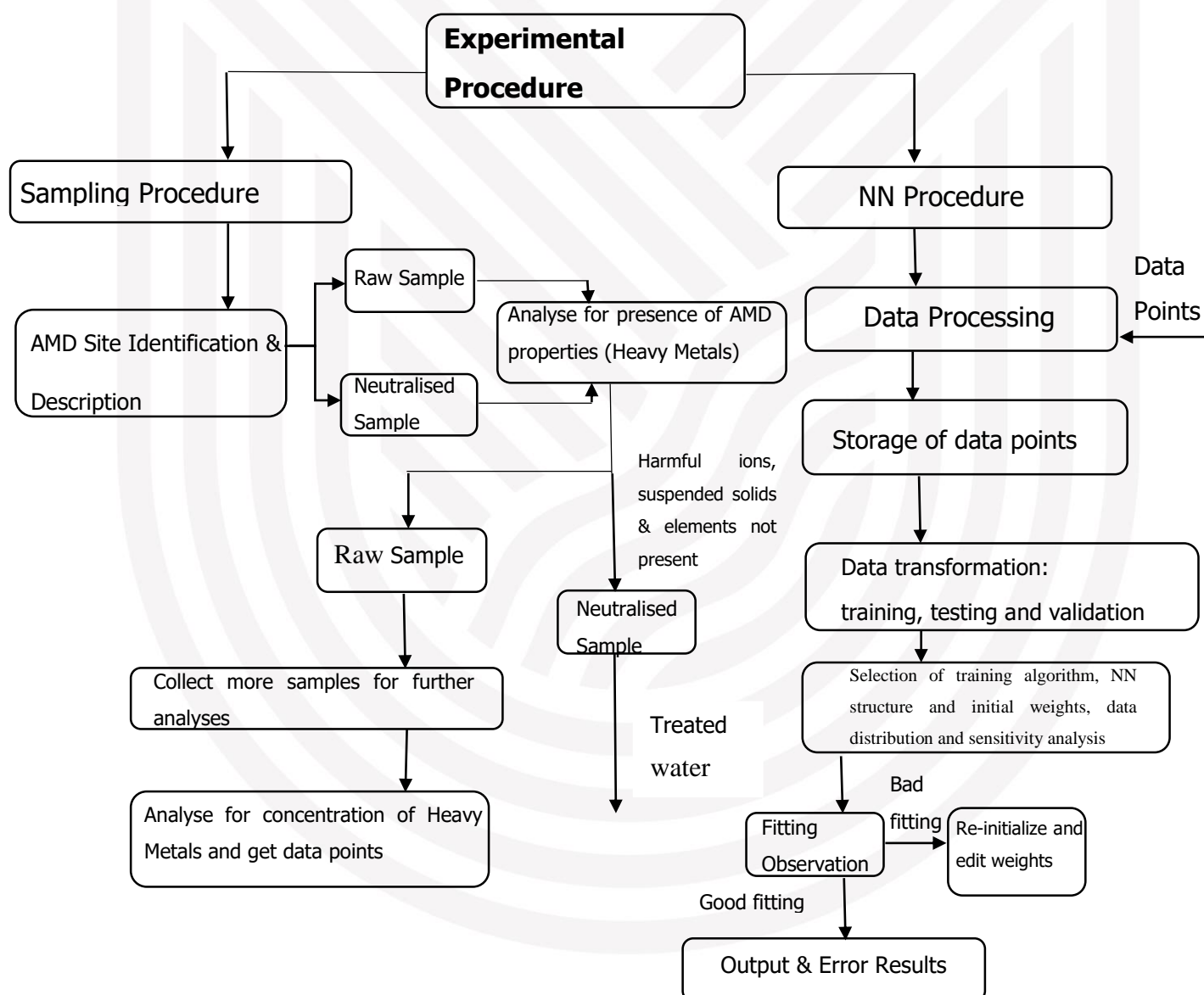


Figure 4: Diagram indicating the flow of the experimental process



### 3.2.1 Site Identification and Sampling Procedure

#### AMD Site Identification

The Sibanye Western Basin AMD Plant was chosen for this research. It is 53,5 km (47 minutes) away from the Vaal University of Technology which was convenient for sample collection. This plant was chosen among the three areas which McCarthy (2011), did a report on in December 2010. It stated that the primary focus was on the immediate problems caused by gold mining and in particular the Western Basin (Krugersdorp area), the Eastern Basin (Brakpan, Springs, and Nigel area) and the Central Basin (Roodepoort to Boksburg) which are now defunct mines. The site of AMD sampling was identified based on the concept that every mining area that releases AMD must send it to a plant to be treated to the compliance standards before releasing the water. The plant receives the acid water from different mines with different ores containing different mineralogical and chemical properties around the western area.

#### Site Description

Samples were taken at the Sibanye Western Basin AMD plant located in Randfontein. The coordinates of the location: 26.1341°S, 27.7162°E.



Figure 5: Map of the Sibanye Western Basin AMD Plant in Randfontein

Sibanye Western Basin AMD Treatment Plant is located in Randfontein, which is a gold mining city in the West Rand that is 40 km west of Johannesburg in the Gauteng province. The



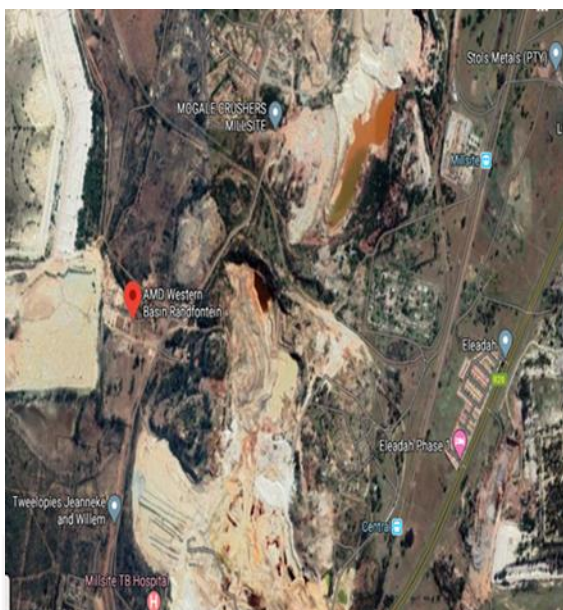


Figure 6: Satellite representation of the Sibanye Western Basin AMD Plant in Randfontein map

main access road to the plant is the R28 provincial route that connects Krugersdorp with Vereeniging through Randfontein. It receives AMD from West Rand Mine Shaft No. 9.

### Sample Collection (Raw and Neutralised Samples)

The raw samples were collected from the pipeline where acid water enters the treatment plant (influent). The raw sample is the acid water prior to any chemical addition. The point of sample collection was opened and water was allowed to run for 10 minutes. The samples were then taken using 2L bottles and immediately stored in the dark (cooler box).

The water sample looked like pure water until it was allowed to stand during storage. Further oxidation of dissolved  $\text{Fe}^{3+}$  ions to form ferric ions took place in the sample and formed ferric ions. The original colour of the wastewater samples changed to brownish and reddish. Thereafter, hydrolysis of  $\text{Fe}^{3+}$  with water occurred to form the solid  $\text{Fe}(\text{OH})_3$  (ferrihydrite) which is orange-red in colour, and release additional acidity. This reaction is pH-dependent and under very acidic conditions of less than about pH 3.5, the solid mineral does not form and  $\text{Fe}^{3+}$  remains in the solution. However, the sample pH was about 4, which is a higher value, and a precipitate, “yellow boy”, was formed (Amanda, 2008). The neutralised sample was taken from an area in the plant where treatment had already taken place by adding 95%  $\text{Ca}(\text{OH})_2$  for neutralisation.



Figure 7: Images of raw and neutralised samples from AMD treatment plant

### Analysis for AMD properties and analytical techniques

- Inductively Coupled Plasma - Optical Emission Spectrometry (ICP-OES) analysis

The acid mine water samples were submitted to Setpoint laboratories in Johannesburg for the ICP-OES analysis, using a model number Varian 700-ES. The water samples were subjected to ICP-OES analysis to determine the concentrations of inorganic elements contained in these samples. The prepared standards of inorganic elements to be detected were used to calibrate the ICP-OES equipment for the ICP-OES analysis of the selected inorganic elements (TEs, lighter inorganic elements and hazardous heavy elements) in the leachate samples (Olesik, 1994).

- Ion Chromatography (IC analysis)

A 20  $\mu\text{L}$  sample was injected into a Metrosep A Supp 4-250/4 anion-exchange column (stationary phase), which was held at 25  $^{\circ}\text{C}$ , with a pressure of 5.83 MPa and a flow rate of 1.00 ml/min. The IC analysis of the sample was carried out under isocratic conditions using disodium carbonate ( $\text{Na}_2\text{CO}_3$ ) (1.8 mmol/L) and sodium hydrogen carbonate ( $\text{NaHCO}_3$ ) (1.7 mmol/L) as the mobile phase with a pH of 10.30. Different standards were used during the IC

analysis including fluoride 2.0 mg/L, chloride 2.0 mg/L, nitrite 5.0 mg/L, bromide 10.0 mg/L, and nitrate 10.0 mg/L.

- EC, TDS, and pH value measurements

The electrical conductivity (EC), which indicates the levels of salinity of the water, the TDS and the pH of the water samples were recorded using a Hana HI 991301 pH meter with a portable EC/pH/TDS/temperature probe.

- NN model

All the above were identified in the two initial raw samples as well as the two neutralised samples which were found free of harmful ions, suspended solids and metals, which meant that the acid water was treated. Twenty-eight (28) more samples were collected to analyse for the same properties as mentioned earlier to attain their concentrations and get data points (results of analysis) to be used on the MATLAB NN Software Toolbox.

The input variables for the NN model were selected based on the physical and chemical characteristics that have greater impact on AMD. These characteristics appear mostly in water that contains heavy metals as they are considered to have most dependence on heavy metals. The targets were chosen based on the heavy metals that were high in concentration in the sample taken and are considered unhealthy for service water and needed to be removed before AMD is released to the public. The input variables identified were pH,  $\text{SO}_4^{2-}$ , and TDS while Zn, Fe, Mn, Si, and Ni were chosen as targets.

The decision to select Zn, Fe, Mn, Si, and Ni was based on the fact that they were found to be in high concentrations in the Western Basin AMD Plant samples and according to literature, Zn can contribute to signs of nausea, vomiting, anaemia, and cholesterol problems in human beings. Fe and Mn form part of heavy metals that can reduce the developmental growth of aquatic species as well as increase anomalies in development, while Ni forms part of metals that are considered potentially carcinogenic. Elemental silicon was also found but it is chemically inactive and therefore the property that causes lung tissue fibrosis is lacking. However, laboratory animals have been found to experience slight pulmonary lesions due to intra-tracheal injections of silicon dust. Chronic respiratory effects are likely to be caused by Si (LennTech, 1998-2020).

### **3.2.2 Neural Network Procedure**

#### **Data processing**

A database is critical when modelling a NN. In the first part, the database was generated by collecting a large number of data points from the experimental data. After evaluating all the experimental results, the collected data were arranged in a set of input vectors as a column in a matrix. Then another set of target vectors were arranged (the correct output vectors for each of the input vectors) to a second matrix in an MS Excel sheet. The input variables were pH,  $\text{SO}_4^{2-}$ , and TDS. The corresponding Zn, Fe, Mn, Si, and Ni were used as targets. To ensure that all variables in the input data were important, principal component analysis (PCA) was performed as an effective procedure for the determination of input parameters. In this dissertation, a multiple-layered perceptron (MLP) type BPNN was used for modeling. All the steps, taken to model the system, can be summarised as follows:

- Step 1: The collected and integrated data points which were the result of the laboratory analyses were stored in a separate data file.
- Step 2: Data transformation was done before starting the network training. The pre-processed data was randomly divided by input vectors and target vectors into three different sets - training, testing and validation.
- Step 3: The developed MATLAB programme (NN Toolbox V4.0 of MATLAB mathematical software) was used for data transformation, network construction, network training, and selecting the best model.

The NN model comparison was mainly used to choose the optimum number of neurons in the hidden layer and identify the type of transfer functions to use in each layer. The performance of the NN during training was measured based on the mean square error.

#### **NN design procedure**

Four important aspects that must be determined in the design procedure of NNs are: (1) selection of the BP training algorithm, (2) data distribution, (3) selection of the NN structure, and (4) selection of the initial weight.

#### **Selection of inputs, targets and functions**

The data points which were the results of the laboratory analyses, were exported to the NN software on Matlab. The inputs (3) and targets (5) were defined from the exported data. Selections of training, adaptation learning, and performance functions were done.

### **Train NN using information and parameters**

The training was done using the input and target as training information. The parameters included information such as epochs, goal, time and showing of command line.

### **Trial and error**

Testing of the NN was done using the parameters mentioned earlier as well as the gradient. The validation check parameter was used to check the validity of the NN and overall data regression, which tells the plots of the NN. Fitting was observed. If the fitting was over or under, then there were re-initialising and editing of weights. The cycle of training, testing, validation and regression was done until the fitting was good. When the fitting was good, the output and error results were retrieved, and the targets and outputs were compared.



## Chapter Summary

This chapter explained the actual experimental process, data processing followed to predict heavy metals in AMD, and the NN design procedure. The data generated were used to create the network and the use of the MATLAB NN Toolbox software was explained. It showed the procedure from the process of identifying an area where AMD water is found, how this area was identified, as well as the confirmation of the water as AMD. The process also showed how the software uses the laboratory data to apply algorithms, transfer functions and perform trial and error calculations to determine the output results and errors. These results were then compared to the target values that were found in the laboratory results.



## Chapter 4: Results and Discussion

### 4.1 Identification of AMD and analysis of raw AMD and treated AMD samples

The most important action in the initial stage was to determine if the collected samples from the chosen site were indeed AMD. The water characteristics results of the raw samples and samples treated with  $\text{Ca}(\text{OH})_2$  are shown in Table 2. The results are of the ten representative samples and the other 20 can be seen in Appendix. The results obtained indicated that the lowest recorded pH of the raw AMD was 2.57 and the sulphate content was found to be between 1334 mg/L (minimum) and 1634 mg/L (maximum), which is very high. A measure above 600 mg/L of sulphate concentration is considered to be harmful to the human health (Moodely et al., 2017). This confirms that the samples analysed were indeed AMD. According to literature by Moodley et al. (2017) AMD is generally characterised by low pH, high heavy metal content, and high salinity, but the sulphate and metal concentrations in the water vary based on the mine (Moodely et al., 2017).

Samples treated with  $\text{Ca}(\text{OH})_2$  were of cleaner standards. The data showed an increase in pH from 2.57 to a maximum of 9 due to the addition of  $\text{Ca}(\text{OH})_2$ . This also led to an increase in the total alkalinity of the treated samples due to the addition of Ca. An insignificant reduction in TDS was observed in the neutralised solutions when compared to the raw solution in the samples, which means that the treatment of AMD had very little impact in reducing TDS. This can be attributed to the fact that ions (Al, Ag, Cr, Mo, Fe, and Pb) react with  $\text{OH}^-$  from the added  $\text{Ca}(\text{OH})_2$  with pH of 7.9 and 8.26 to form metal hydroxide precipitates. Conductivity indicates the level of salinity of water and the AMD conductivity was high due to high salinity. The addition of  $\text{Ca}(\text{OH})_2$  increases pH and lowers the salinity of the AMD and therefore, the conductivity of the treated solution also decreased as seen in Table 2.

Table 2: Water characteristics analysis results for AMD (raw and treated) at Sibanye Western Basin AMD Plant

- Raw AMD: R AMD; Treated AMD: T AMD

Water Characteristics	SAMPLE NUMBERS																			
	1		2		3		4		5		6		7		8		9		10	
	R AMD	T AMD	R AMD	T AMD	R AMD	T AMD	R AMD	T AMD	R AMD	T AMD	R AMD	T AMD	R AMD	T AMD	R AMD	T AMD	R AMD	T AMD	R AMD	T AMD
<b>Conductivity (mS/m @ 25°C)</b>	362	331	364	327	487	371	489	374	487	385	485	388	478	365	472	369	481	383	479	388
<b>pH</b>	4.17	7.90	4.17	8.26	2.66	8.69	2.64	8.81	2.64	8.34	2.65	8.45	2.66	9.00	2.62	9	2.66	8.52	2.6	8.64
<b>Sulphate (mg/L)</b>	1627	1510	1634	1520	1547	1430	1565	1437	1562	1465	1556	1482	1550	1436	1544	1418	1573	1515	1558	1518
<b>Total Alkalinity (mg/L CaCO<sub>3</sub>)</b>	< 0.10	25.8	< 0.10	20.2	< 0.10	25.8	< 0.10	25.2	< 0.10	24.6	< 0.10	24.8	< 0.10	24.8	<0.10	24.8	<0.10	25.6	<0.10	24.4
<b>TDS (mg/L @ 180°C)</b>	2357	2153	2370	2127	3110	2377	3130	2397	3110	2463	3103	2480	3057	2337	3027	2367	3070	2457	3067	2477

Heavy metals were identified, with Zn, Fe, Mn, Si, and Ni in high concentrations. A heavy metals analysis was done on the raw and treated AMD samples to determine if the heavy metals were removed by the neutralisation process in order to get the water to cleaner standards. Table 3 shows that in the presence of oxygen, ferrous iron was oxidised to ferric iron which precipitated at a pH of about 3.5. Ferric hydroxide formed a yellowish-orange solid, known as yellow boy, which usually precipitates at a pH greater than 3.5. Therefore, when the pH increased to 7.9 and 8.26, ferric hydroxide was precipitated. In all samples, Fe went from high concentrations to <10.0 which is below detection. This can be seen in sample 1, where the initial concentration of Fe went from 289 mg/L to <10.0 mg/L.

Mn precipitation was variable due to its many oxidation states, but it generally precipitates at a pH of 9.0 to 9.5. In samples that reached a pH of 9.0, it was precipitated as shown in Table 3. In samples that did not reach a pH of 9.0, Fe precipitation largely removed Mn from the water at a pH of 8 due to co-precipitation, because the Fe concentration in the water was much greater than the Mn content. Some of the Mn remained as dissolved Mn but in very small concentrations.

Complete precipitation of Zn occurs at pH 10.1. However, the pH of the samples was only raised from 7.0 to 9.0. At these pH values, most of the Zn forms zinc hydroxide and precipitates out of the solution while some of the Zn remains as dissolved Zn. In sample 1, for instance, the concentration of Zn was reduced from 0.33 mg/L to 0.07 mg/L. The same concept applies for Ni, which completely precipitates at pH 10.8 to 11. At a pH between 7.0 and 9.0, most of the Ni forms nickel hydroxide and precipitates out of the solution leaving the rest as dissolved Ni. In sample 1, for instance, the concentration of Ni was reduced from 0.521 mg/L to 0.0272 mg/L.

Table 3: Heavy metal analysis results for AMD (raw and treated) at Sibanye Western Basin AMD Plant

- **Raw AMD: R AMD; Treated AMD: T AMD**

Heavy Metals (Mg/L)	SAMPLE NUMBERS																			
	1		2		3		4		5		6		7		8		9		10	
	R AMD	T AMD	R AMD	T AMD	R AMD	T AMD	R AMD	T AMD	R AMD	T AMD	R AMD	T AMD	R AMD	T AMD	R AMD	T AMD	R AMD	T AMD	R AMD	T AMD
Zn	0.33	0.07	0.36	0.08	0.28	<0.06	0.16	<0.06	0.18	<0.06	0.18	<0.06	0.19	<0.06	0.20	<0.06	0.23	<0.06	0.22	<0.06
Fe	289	< 0.10	289	< 0.10	37.7	< 0.10	41.1	< 0.10	38.8	< 0.10	38.3	< 0.10	41.3	< 0.10	35.4	< 0.10	39.6	< 0.10	39.8	< 0.10
Mn	45	0.0533	46.5	0.0502	38.2	0.0272	39.2	0.0139	39.3	0.0383	39.4	0.0332	39.4	0.0155	39.6	0.0676	39.7	0.0159	40.0	0.0161
Ni	0.521	0.0272	0.490	0.0203	0.452	0.0195	0.443	0.0201	0.450	0.0218	0.443	0.0437	0.594	0.0210	0.586	0.0248	0.558	0.0194	0.540	0.0229
Si	8.56	0.37	8.58	0.38	9.48	0.49	9.46	0.47	9.52	0.57	9.86	0.54	9.38	0.46	9.54	0.44	9.44	0.43	9.43	0.43

Ca and Na were identified. The addition of the neutralising agent led to an increase in Ca concentration and this can be seen in sample 1 where Ca increased from 683 mg/L to 872 mg/L. Table 4 shows that other elements such as Li, Na, K, and Al, remained in the same range and that there was no significant increase or decrease in their concentrations when the neutralising agent was added. Al was even below the standards of detection. Trace metals that were identified include Ag, As, Cd, Co, Cr, Cu, Mo and Pb. These results can be found in Appendix A. The trace metals were found in very small concentrations which make them non-hazardous.



Table 4: Elemental analysis results for AMD (raw and treated) at Sibanye Western Basin AMD Plant

- Raw AMD: R AMD; Treated AMD: T AMD

Elements  Mg/L	SAMPLE NUMBERS																			
	1		2		3		4		5		6		7		8		9		10	
	R AMD	T AMD	R AMD	T AMD	R AMD	T AMD	R AMD	T AMD	R AMD	T AMD	R AMD	T AMD	R AMD	T AMD	R AMD	T AMD	R AMD	T AMD	R AMD	T AMD
Li	0.12	0.12	0.12	0.12	0.12	0.12	0.12	0.12	0.12	0.12	0.13	0.12	0.12	21.2	0.12	0.11	0.11	0.11	0.11	0.12
Na	170	180	175	175	153	162	156	157	158	158	163	153	154	157	155	151	144	144	147	154
K	19.5	20.8	20.3	20.4	20.2	21.1	20.6	20.8	20.8	21.2	21.5	20.5	20.5	21.2	20.8	20.6	19.5	18.2	19.9	19.7
Ca	683	872	709	856	658	763	683	751	674	789	685	763	656	749	622	719	621	687	627	753
Al	< 0.15	< 0.15	< 0.15	< 0.15	< 0.15	< 0.15	< 0.15	< 0.15	< 0.15	< 0.15	< 0.15	< 0.15	< 0.15	< 0.15	< 0.15	< 0.15	< 0.15	< 0.15	< 0.15	< 0.15
Mg	183	168	187	168	178	147	180	145	180	150	186	147	182	136	182	130	173	152	176	156
Be	<0.001	<0.001	<0.001	<0.001	0.0018	<0.001	0.0012	<0.001	0.0000	<0.001	0.0012	<0.001	0.0013	<0.001	0.002	<0.001	0.001	<0.001	0.001	<0.001
			1	01					8						0		2		3	



## 4.2 Application of NN

According to Toma et al. (2004), to design NN, the important aspects must be determined: (1) selection of the backpropagation (BP) training algorithm, (2) data distribution, (3) selection of the NN structure, and (4) selection of the initial weight.

### 4.2.1 Selection of the BP Training Algorithm

Ten BP training algorithms were compared, as illustrated in Table 5, to select the best suited BP training algorithm. The NNTool was used where the laboratory results of the samples were imported into the tool. In all the BP training algorithms, a three-layer NN with a tangent sigmoid transfer function (*tansig*) at the hidden layer and a linear transfer function (*purelin*) at the output layer were used. The chosen training algorithm was the Levenberg-Marquardt back-propagation (*trainlm*) because it had the smallest MSE of 0.00041, meaning the error of this algorithm was very low. The MSE is elaborated in Equation (18). The line of best fit for the data set used in this experiment, also known as BLE, was described by Equation (19). The BLE that was chosen after training and testing was  $y = x + 1.4$ . It gave a clear straight line with the values for training, validation, and test RMS at 0.99908.

Table 5: Comparison of 10 BP algorithms

BP Algorithms	Function	MSE	BLE
1. Batch gradient descent.	<i>traingd</i>	0.54628	$y = 0.94x - 11$
2. Batch gradient descent with momentum.	<i>traingdm</i>	0.60734	$y = 0.94x - 11$
3. BFGS quasi-Newton back-propagation.	<i>trainbfg</i>	0.07108	$y = x + 4.5$
4. Fletcher-Reeves conjugate gradient back-propagation.	<i>traincgf</i>	0.15623	$y = x + 2.4$
5. Levenberg-Marquardt back-propagation.	<i>trainlm</i>	0.00041	$y = x + 1.4$
6. One step secant back-propagation.	<i>trainoss</i>	0.17672	$y = x - 1.9$
7. Polak-Ribiere conjugate gradient back-propagation.			

8. Powell-Beale conjugate gradient back-propagation.	<i>traincgp</i>	0.12782	$y = x + 2.5$
9. Scaled conjugate gradient back-propagation.	<i>traincgb</i>	0.15873	$y = 0.99x + 0.86$
10. Variable learning rate back-propagation.	<i>trainscg</i>	0.13185	$y = x - 1.3$
	<i>traingdx</i>	0.64620	$y = x + 0.78$

#### 4.2.2 Data Distribution

The NN model was based on the selected BP algorithm, Levenberg-Marquardt back-propagation (*trainlm*), for the experimental data. This was applied to train the NN. During training, the output matrix was computed by a forward pass (feed-forward backpropagation NN) in which the input matrix was propagated forward through the network to compute the output value of each unit. The output matrix was then compared with the desired matrix which results in an error signal for each output unit. To minimise the error, appropriate adjustments were made for each of the weights of the network. The training was stopped after iterations for the LMA where the differences between training errors and validation errors were starting to increase.

Eight iterations of training were performed with different weights being adjusted. Figures 8 to 17 illustrate the training, validation, and test MSE for the LMA after the eight adjustment and the difference in error was found to increase for all ten algorithms.

1. The Batch gradient descent (*traingd*) algorithm resulted in an RMS of 0.99085 during training, 0.99916 during validation, 0.99934 during testing and a summary of all the stages resulted in an RMS of 0.99315. The training parameters for this algorithm were the following:

Show window: true
Show command line: false
Show: 25
Epoch: 1000
Time: Inf
Goal: 0
Min_grad: 1e-05
Max_fail: 6
Ir: 0.01
Show window: true

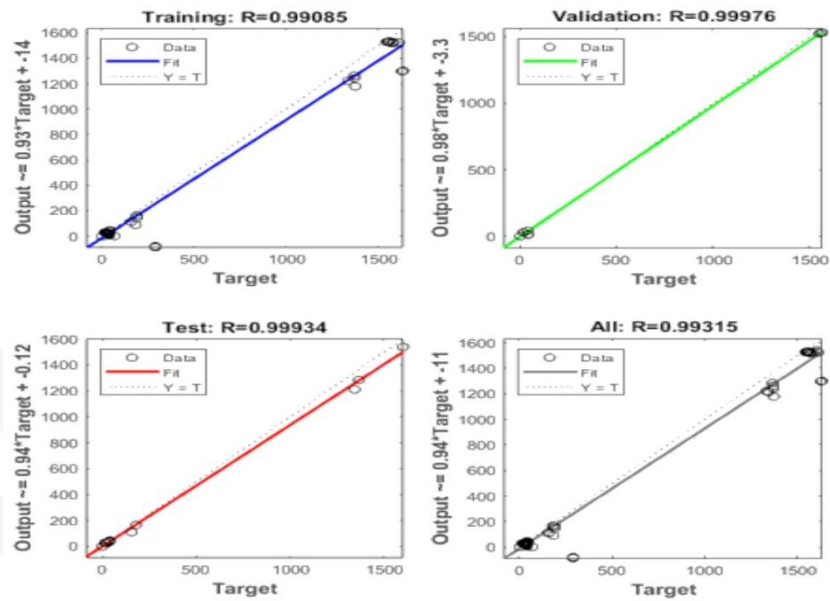


Figure 8: Training, validation, and test MSE for the LMA for the Batch gradient descent (*traingd*) algorithm

2. The Batch gradient descent with momentum (*traingdm*) algorithm resulted in an RMS of 0.99085 during training, 0.99976 during validation, 0.99934 during testing and a summary of all the stages resulted in an RMS of 0.99315. The training parameters for this algorithm were the following:

Show window: true
Show command line: false
Show: 25
Epoch: 1000
Time: Inf
Goal: 0
Min_grad: 1e-05
Max_fail: 6
Ir: 0.01
mc: 0.9

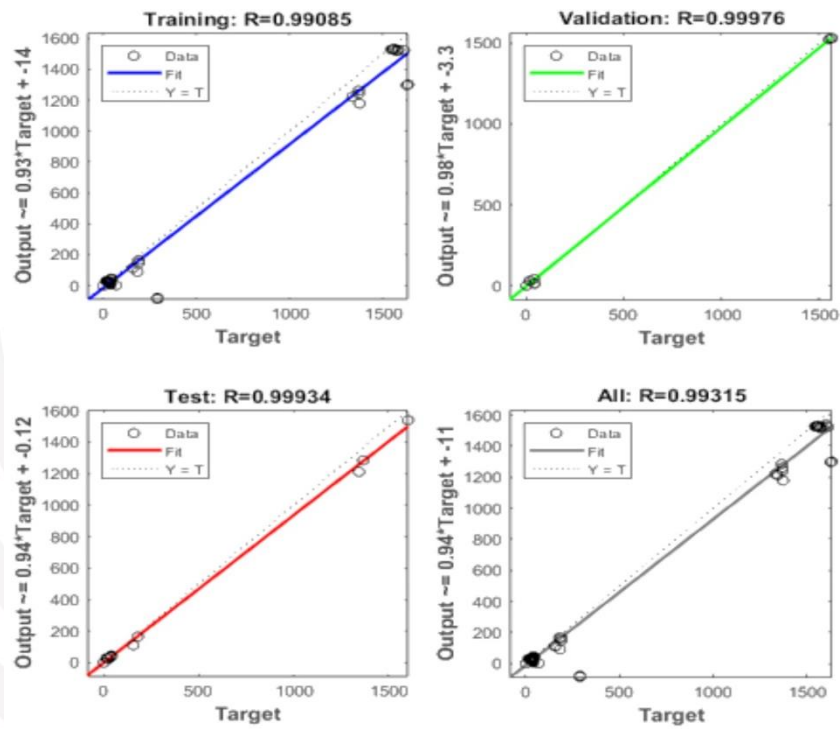


Figure 9: Training, validation, and test MSE for the LMA for the Batch gradient descent with momentum (*traingdm*) algorithm

3. The BFGS quasi-Newton back-propagation (*trainbfg*) algorithm resulted in an RMS of 0.99898 during training, 0.99998 during validation, 0.99875 during testing and a

summary of all the stages resulted in an RMS of 0.99906. The training parameters for this algorithm were the following:

Show window: true	searchFcn: 'srchbac'	bmax: 26
Show command line: false	scale_tol: 20	batch_frag: 0
Show: 25	alpha: 0.001	
Epoch: 1000	beta: 0.1	
Time: Inf	delta: 0.01	
Goal: 0	gama: 0.1	
Min_grad: 1e-06	low_lim: 0.1	
Max_fail: 6	up_lim: 0.5	
Ir: 0.01	max_step: 100	
mc: 0.9	min_step: 1e-06	

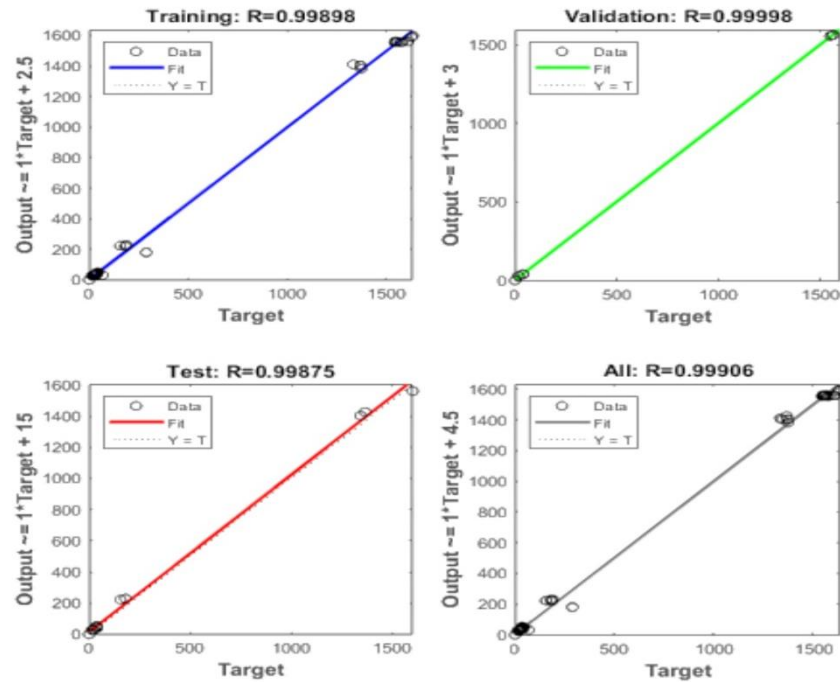


Figure 10: Training, validation, and test MSE for the BFGS quasi-Newton back-propagation (*trainbfg*) LMA for the algorithm

4. The Fletcher-Reeves conjugate gradient back-propagation (*traincgf*) algorithm resulted in an RMS of 0.9989 during training, 0.99998 during validation, 0.99926 during testing and a summary of all the stages resulted in an RMS of 0.99908. The training parameters for this algorithm were the following:

Show window: true	searchFcn: 'srchbac'	max_step: 100
Show command line: false	scale_tol: 20	min_step: 1e-10
Show: 25	alpha: 0.001	bmax: 26
Epoch: 1000	beta: 0.1	batch_frag: 0
Time: Inf	delta: 0.01	
Goal: 0	gama: 0.1	
Min_grad: 1e-10	low_lim: 0.1	
Max_fail: 6	up_lim: 0.5	

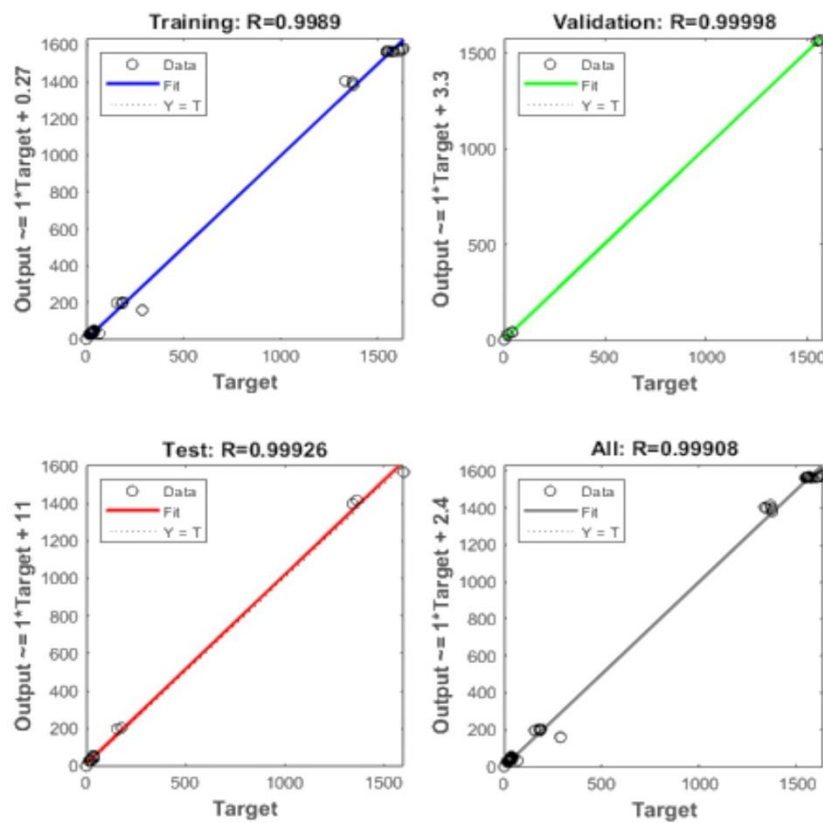


Figure 11: Training, validation, and test MSE for the LMA for the Fletcher-Reeves conjugate gradient back-propagation (*traincgf*) algorithm



5. The One step secant back-propagation (*trainoss*) algorithm resulted in an RMS of 0.99814 during training, 0.99416 during validation, 0.99989 during testing and a summary of all the stages resulted in an RMS of 0.9978. The training parameters for this algorithm were the following:

Show window: true	searchFcn: 'srchbac'	max_step: 100
Show command line: false	scale_tol: 20	min_step: 1e-06
Show: 25	alpha: 0.001	bmax: 26
Epoch: 1000	beta: 0.1	
Time: Inf	delta: 0.01	
Goal: 0	gama: 0.1	
Min_grad: 1e-10	low_lim: 0.1	
Max_fail: 6	up_lim: 0.5	

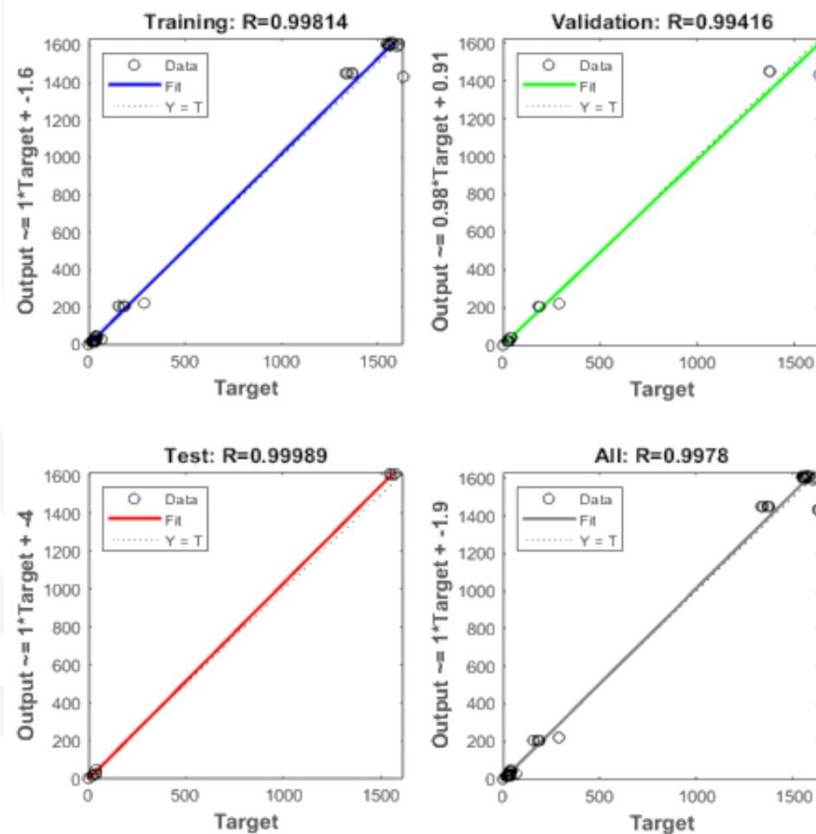


Figure 12: Training, validation, and test MSE for the LMA for the One step secant back-propagation (*trainoss*) algorithm

6. The Polak-Ribiere conjugate gradient back-propagation (*traincgp*) algorithm resulted in an RMS of 0.99897 during training, 0.99998 during validation, 0.99929 during testing and a summary of all the stages resulted in an RMS of 0.9913. The training parameters for this algorithm were the following:

Show window: true	searchFcn: 'srchbac'	max_step: 100
Show command line: false	scale_tol: 20	min_step: 1e-06
Show: 25	alpha: 0.001	bmax: 26
Epoch: 1000	beta: 0.1	
Time: Inf	delta: 0.01	
Goal: 0	gama: 0.1	
Min_grad: 1e-10	low_lim: 0.1	
Max_fail: 6	up_lim: 0.5	

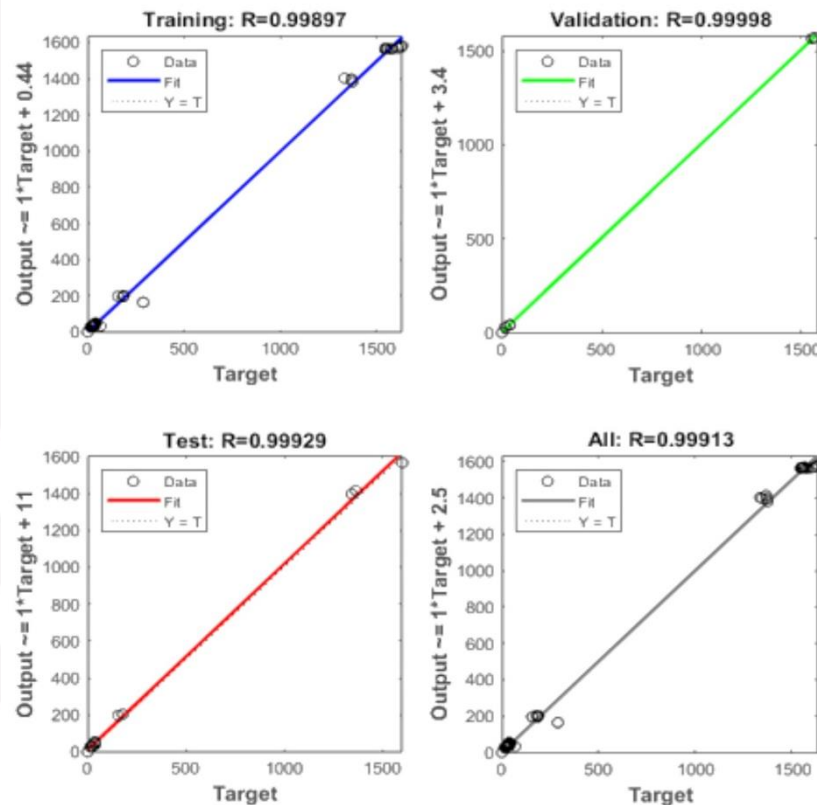


Figure 13: Training, validation, and test MSE for the LMA for the Polak-Ribiere conjugate gradient back-propagation (*traincgp*) algorithm

7. The Powell-Beale conjugate gradient back-propagation (*traincgb*) algorithm resulted in an RMS of 0.99944 during training, 0.99995 during validation, 0.999955 during testing and a summary of all the stages resulted in an RMS of 0.9994. The training parameters for this algorithm were the following:

Show window: true	searchFcn: 'srchbac'	max_step: 100
Show command line: false	scale_tol: 20	min_step: 1e-06
Show: 25	alpha: 0.001	bmax: 26
Epoch: 1000	beta: 0.1	
Time: Inf	delta: 0.01	
Goal: 0	gama: 0.1	
Min_grad: 1e-10	low_lim: 0.1	
Max_fail: 6	up_lim: 0.5	

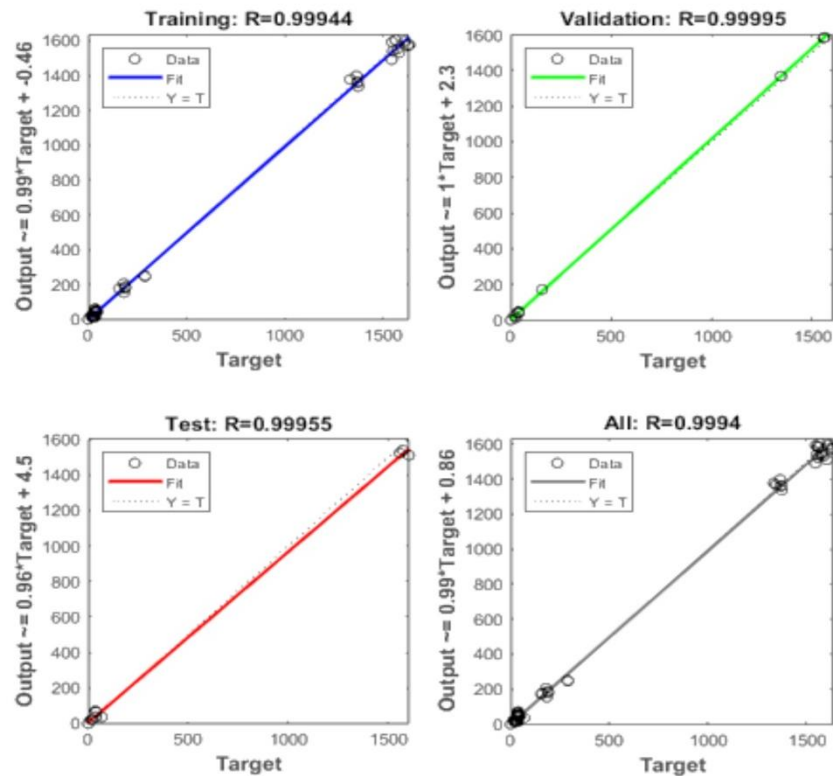


Figure 14: Training, validation, and test MSE for the LMA for the Powell-Beale conjugate gradient back-propagation (*traincgb*) algorithm

8. The Scaled conjugate gradient back-propagation (*trainscg*) algorithm resulted in an RMS of 0.99978 during training, 0.99994 during validation, 0.99996 during testing and a summary of all the stages resulted in an RMS of 0.99982. The training parameters for this algorithm were the following:

Show window: true	sigma: 5e-05
Show command line: false	lambda: 5e-07
Show: 25	
Epoch: 1000	
Time: Inf	
Goal: 0	
Min_grad: 1e-10	
Max_fail: 6	

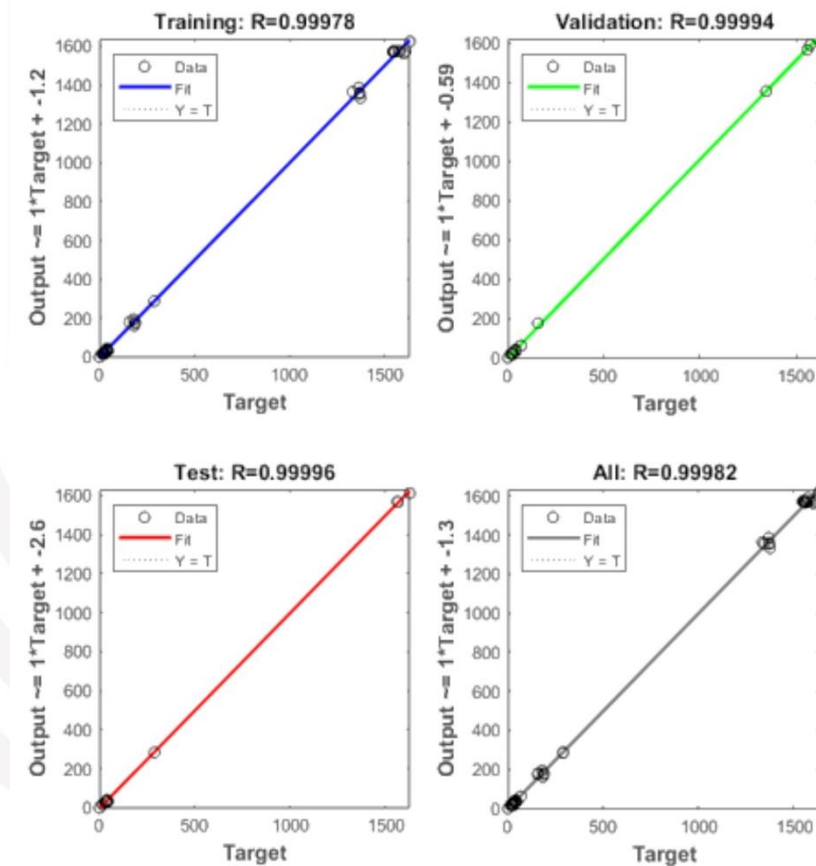


Figure 15: Training, validation, and test MSE for the LMA for the Scaled conjugate gradient back-propagation (*trainscg*) algorithm

9. The Variable learning rate back-propagation (*traingdx*) algorithm resulted in an RMS of 0.99894 during training, 0.99995 during validation, 0.99968 during testing and a summary of all the stages resulted in an RMS of 0.9992. The training parameters for this algorithm were the following:

Show window: true	Ir: 0.01
Show command line: false	Ir_inc: 0.05
Show: 25	Ir_dec: 0.7
Epoch: 1000	max_perf_inc: 0.04
Time: Inf	mc: 0.9
Goal: 0	
Min_grad: 1e-10	
Max_fail: 6	

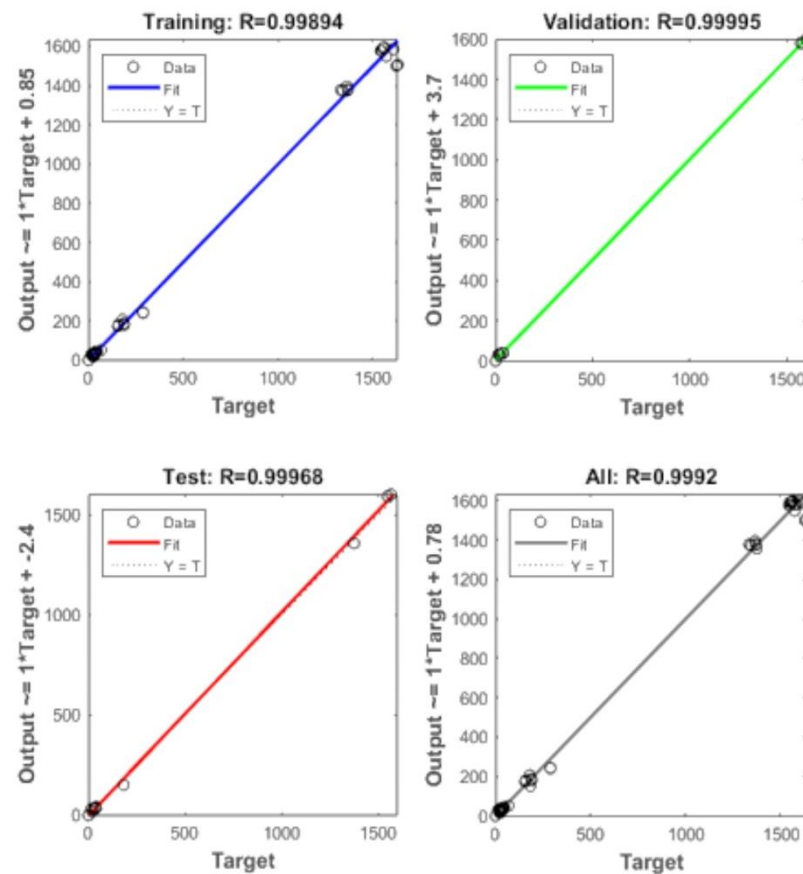


Figure 16: Training, validation, and test MSE for the LMA for the Variable learning rate back-propagation (*traingdx*) algorithm

10. The Levenberg-Marquardt back-propagation (trainlm) algorithm resulted in an RMS value of 0.99993 during training, 0.99998 during validation, 0.9993 during testing and a summary of all the stages resulted in an RMS of 0.99984. This means that the output predicted by the network is nearly an exact fit with the output from the laboratory analysis and this is shown by the MSE of 0.00041. This algorithm was found to be the one that resulted in the optimum structure because it had the smallest MSE value and the BLE showed better fit than the other algorithms. This means that the ideal algorithm to use in training the NNTool for the prediction of heavy metals in mine water was the Levenberg-Marquardt back-propagation. The results of the output predicted by the network will be of great closeness to the output from the laboratory analysis by an MSE value of 0.00041. The training parameters for this algorithm were the following:

Show window: true	mu: 0.001
Show command line: false	mu_dec: 0.1
Show: 25	mu_inc: 10
Epoch: 1000	mu_max: 10000000000
Time: Inf	
Goal: 0	
Min_grad: 1e-10	
Max_fail: 6	

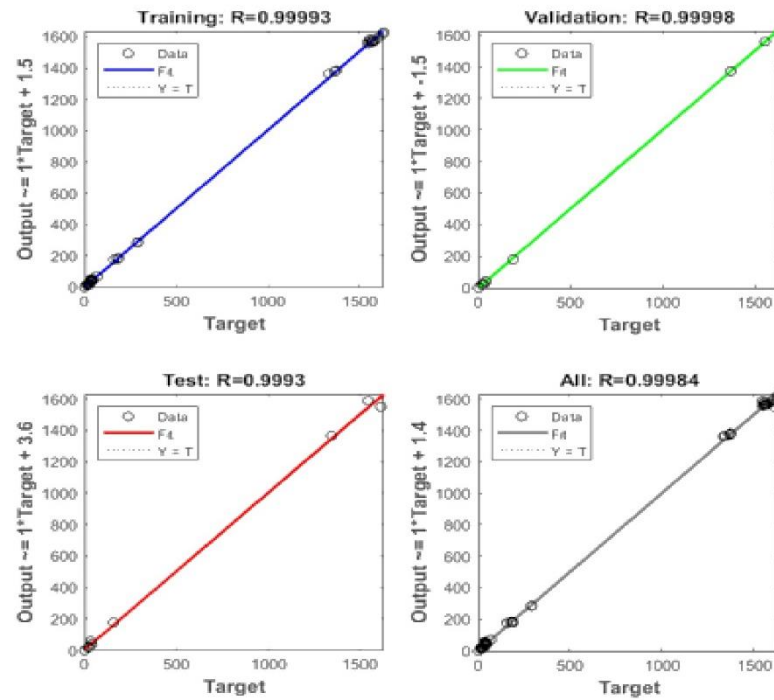


Figure 17: Training, validation, and test MSE for the LMA for the Levenberg-Marquardt back-propagation (trainlm) algorithm



### 4.2.3 Selection of NN Structure

For the best performance of the NN structure to be determined, it was necessary for the optimal network architecture to be defined. The number of hidden layers and the number of neurons in it were determined based on the minimum value of MSE of the training and prediction set. The minimum value of MSE was 0.00041 using the Leven Levenberg-Marquardt back-propagation (*trainlm*). Figure 18, shows the optimal structure directly from the MATLAB NNtool found with one hidden layer and five neurons.

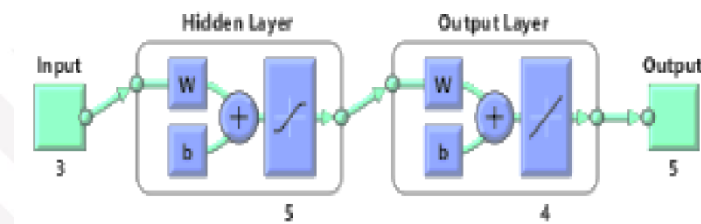


Figure 18: Optimal NN structure from MATLAB NNtool

The network was found to be fully connected. This means that there was a connection of every neuron in each layer to every neuron in the next layer. The NN structure was named, based on the number of neurons in each layer. Figure 19, shows the optimum NN structure in detail when the Levenberg-Marquardt back-propagation (*trainlm*) is applied on a three-layer NN with a tangent sigmoid transfer function (*tansig*) at the hidden layer and a linear transfer function (*purelin*) at the output layer. There is only one hidden layer that consists of five neurons.

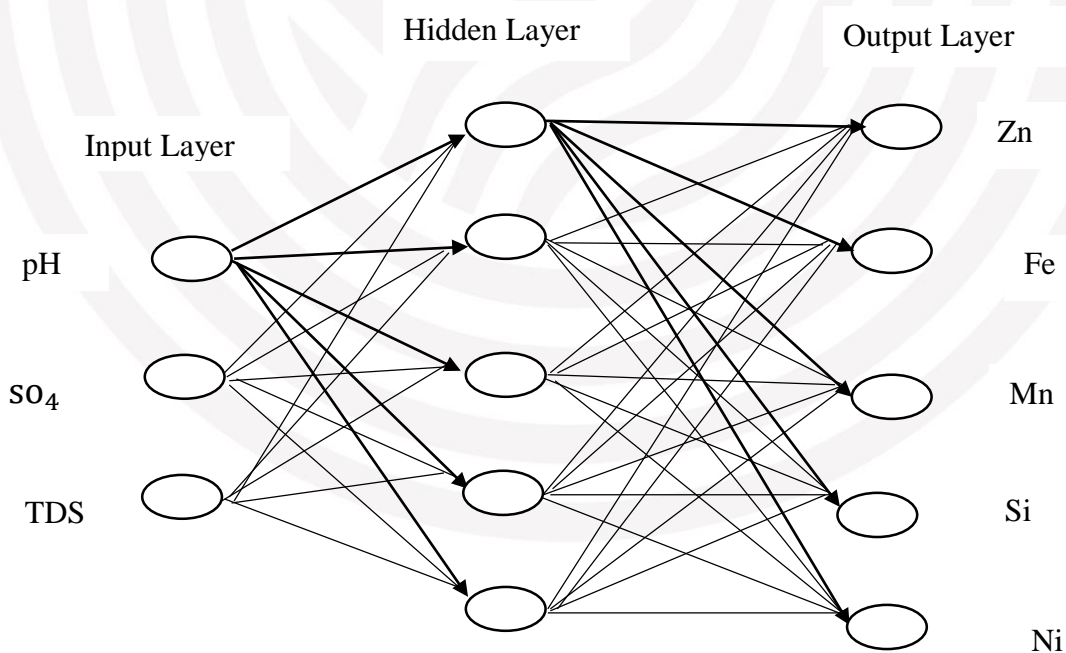


Figure 19: Detailed optimal NN structure using the *trainlm* BP algorithm

#### 4.2.4 Selection of Initial Weight

According to literature, an important problem encountered when training a NN is the determination of the appropriate initial values for the connection weights. These weights are modified during utilisation to satisfy a criterion of performance. A NN basically adds up the signal that comes from its inputs and multiplies them with the correspondent weights. If the result goes beyond the threshold, the neuron can fire and transmit a signal at the output using a transfer function (Vlad, 2004).

The effective weight initiation is associated with performance characteristics such as the time needed to successfully train the network and the generalisation ability of the trained network (Adam et al., 2014). The wrong choice of initial weights can lead to an increase in the training time or can even cause the non-convergence of the training algorithm. To decide on the initial weight for NN training, the Garson equation (Equation 22) was used (Aber et al., 2009).

$$I_j = \frac{\sum_{m=1}^{m=Nh} \left( \left( |W_{jm}^{ih}| / \sum_{k=1}^{Ni} |W_{km}^{ih}| \right) x |W_{mn}^{ho}| \right)}{\sum_{k=1}^{k=Ni} \left\{ \sum_{m=1}^{m=Nh} \left( |W_{km}^{ih}| / \sum_{k=1}^{Ni} |W_{kn}^{ih}| x |W_{mn}^{ho}| \right) \right\}} \quad \text{Equation 22}$$

In equation (22), W is the connection weight. The superscripts 'I' 'h' and 'o' refer to input, hidden and output layers, respectively and subscripts 'k', 'm' and 'n' refer to input, hidden and output neurons, respectively.

The initial weights to layer 1 from input 1 using the Levenberg-Marquardt back-propagation algorithm was: [1.2251; -1.5666; -1.3327; 1.4726; -0.80382; 1.7078; -1.5087; 0.18962; 1.8491; 1.6045; 1.7758; -0.056764; 0.55684; 1.9558; 1.2663]. These weights resulted in the decision to make the Levenberg-Marquardt back-propagation (*trainlm*) algorithm the optimum one because it resulted in the MSE of 0.00041. The combination of this algorithm and weights gave the smallest MSE after testing ten algorithms, meaning the error of this algorithm was very low. These weights also made the training time short and resulted in the BLE after training and testing to be  $y = x + 1.4$ . It gave a clear straight line with the values for training, validation, and test RMS at 0.99908.

## Chapter Summary

In this chapter, it was illustrated how AMD properties were identified in the samples taken from Sibanye Western Basin Treatment Plant. The properties found correspond to the definition of AMD in the literature. Neutralisation using  $\text{Ca}(\text{OH})_2$  proved to be successful in precipitating heavy metals, especially those identified to be problematic, as well as light metals.

The designing of NN for its application focused on four important aspects that had to be determined. Firstly, the selection of the backpropagation (BP) training algorithm, where the optimum algorithm was found to be the Levenberg-Marquardt back-propagation (*trainlm*). Secondly, data distribution, where the optimum algorithm was applied to train the NN. During training, the output matrix was computed by a forward pass (feed-forward backpropagation NN) in which the input matrix was propagated forward through the network to compute the output value of each unit. The output matrix was then compared with the desired matrix. Thirdly, the selection of the NN structure, where a three-layer NN with a tangent sigmoid transfer function (*tansig*) at the hidden layer and a linear transfer function (*purelin*) at the output layer were applied. There was only one hidden layer that consisted of five neurons. Lastly, the selection of the initial weight where Adam et al. (2014) highlighted that the effective weight initiation is associated with performance characteristics such as the time needed to successfully train the network and the generalisation ability of the trained network.

## Chapter 5: Conclusions and Recommendations

### 5.1 Conclusions

The application of NN techniques to predict the heavy metals in AMD from South African mines has been presented. Identification of AMD and heavy metals in AMD was done. AMD is characterised by low pH, high heavy metal content, and high salinity and samples showed these characteristics. The heavy metals that were identified and found in high concentrations in the AMD samples from Sibanye Western Basin AMD Treatment Plant were Zn, Fe, Mn, Si and Ni.

The input, output and hidden layers of the NN structure (application of NN) was done, the appropriate algorithm to train the NN was found, and the NN results (outputs) were compared with the measured concentrations of heavy metals (targets). The BP model had three layers which included the input layer (pH,  $\text{SO}_4^{2-}$ , and TDS), the hidden layer (five neurons) with a tangent sigmoid transfer function (*tansig*) and the output layer (Cu, Fe, Mn and Zn) with a linear transfer function (*purelin*).

The predictions for heavy metals (Zn, Fe, Mn, Si and Ni) using the NN method focusing on a BP forward pass (feed-forward backpropagation NN) with ten different algorithms were presented and compared with the measured data. The mean square error (MSE) value was calculated for ten algorithms and compared to identify the one that is most appropriate for the prediction process and the model by having the lowest value. It was determined that the Levenberg-Marquardt back-propagation (*trainlm*) algorithm resulted in the best fitting during training because it resulted in an MSE value of 0.00041, meaning the error was very low when this algorithm was used. The input data for the NN model were selected based on the physical and chemical characteristics that have greater impact on AMD. These characteristics appear mostly in water that contains heavy metals and they are considered to have the most dependence on heavy metals.

### 5.2 Recommendations

It has been shown that the BP forward pass (feed-forward backpropagation NN) using the Levenberg-Marquardt back-propagation (*trainlm*) algorithm can successfully train the NN to predict heavy metals in AMD. It is recommended that the study be extended to use more input parameters. An increase in parameters should lead to an increase in the accuracy of the study.

The site of the AMD sampling was identified based on the concept that every mining area that releases AMD must send it to a plant to be treated to the compliance standards of releasing the water. The plant receives the acid water from different mines with ores that contain different mineralogical and chemical properties around the western area. It is therefore recommended that continuation of the study should focus on one mine with ore that has similar mineralogy and chemical properties for the NN model to be more accurate.



## References

- Aber, S., Amani-Ghadim, A. R. & Mirzajani, V., 2009. Removal of Cr(VI) from polluted solutions by electrocoagulation: Modeling of experimental results using artificial neural network. *Journal of Hazardous Materials*, 171, pp. 484-490.
- Ahsan , H., Chen, Y., Parvez, F. & Zablotska, L., 2006. Arsenic exposure from drinking water and risk of premalignant skin lesions in Bangladesh: Baseline results from the health effects of arsenic longitudinal study. *American Journal of Epidemiology*, 163(1), pp. 1138-1148.
- Akcil, A. & Koldas, S., 2005. Acid Mine Drainage (AMD): Causes, treatment and case studies. *Journal of Cleaner Production*, 14(2006), pp. 1139-1145.
- Amanda, S., 2008. *Pollution Equipment News*. [Online] Available at: <https://www.pollutionequipmentnews.com/acid-mine-drainage-reduced-with-calcium-hydroxide-lime-slurry> [Accessed 08 02 2020].
- Anon., 2013. *House Plants Experts*. [Online] Available at: <https://www.houseplantsexpert.com/a-z-list-of-house-plants.html> [Accessed 14 04 2020].
- Aubé, B. & Zinck, J., 2003. *Lime Treatment of Acid Mine Drainage in Canada*. Florianópolis, Brazil, Brazil-Canada Seminar on Mine Rehabilitation, pp. 01-13.
- Bangal, C. B., 2009. *Automatic Generation Control of Interconnected Power Systems Using Artificial Neural Network Techniques*. Chennai: PhD Thesis, Bharath University.
- Barakat, M., 2010. New trends in removing heavy metals from industrial wastewater. *Arabian Journal of Chemistry*, 4, pp. 361-377.
- Betrie, G. D., Tesfamariam , S., Morin , K. A. & Sadiq, R., 2012. Predicting copper concentrations in acid mine drainage: a comparative analysis of five machine learning techniques. *Environ Monit Assess*, 185, p. 4171–4182.
- Boruah, D., Thakur, P. K. & Baruah, D., 2016. Artificial Neural Network based Modelling of Internal Combustion Engine Performance. *International Journal of Engineering Research & Technology*, 05(03), pp. 568-577.
- Cavalcante , A. M. et al., 2010. Comparative Evaluation of the pH of Calcium Hydroxide Powder in Contact with Carbon Dioxide (CO<sub>2</sub>). *Materials Research*, 13(01), pp. 1-4.



Chemicool, d., 2017. *chemistry dictionary definition of metalloids*. [Online] Available at: <https://www.chemicool.com/definition/metalloid.html> [Accessed 04 06 2020].

Chibuikwe, G. U. & Obiora, S. C., 2014. Heavy Metal Polluted Soils: Effect on Plants and Bioremediation Methods. *Applied and Environmental Soil Science*, 1, pp. 1-12.

Dodson, M. E., Opitz, B. E. & Serne, R. J., 1984. *Laboratory Evaluation of Limestone and Lime Neutralization of Acidic Uranium Mill Tailings Solution*, Washington D.C: Pacific Northwest Laboratory.

Elçiçek , H., Akdoğlan , E. & Karagöz, S., 2014. The Use of Artificial Neural Network for Prediction of Dissolution Kinetics. *The Scientific World Journal*, 2014(01), pp. 01-09.

Estrela, C., Sydney, G. B., Bammann, L. L. & Oswaldo, F. J., 1994. Study of the biological effect of pH on the enzymatic activity of anaerobic bacteria. *Rev. Fac. Odont. Bauru*, 2(4), pp. 31.

EuroChlor, 2016. *EuroChlor*. [Online] Available at: [https://www.eurochlor.org/wp-content/uploads/2019/03/03-caustic\\_soda.pdf](https://www.eurochlor.org/wp-content/uploads/2019/03/03-caustic_soda.pdf) [Accessed 07 07 2020].

Fard, B. Z., Ghadimi , F. & Fattahi, H., 2017. Use of artificial intelligence techniques to predict distribution of heavy metals in groundwater of Lakan lead-zinc mine in Iran. *Journal of Mining & Environment*, 08(01), pp. 35-48.

Fig, D., 2011. Surfaces and externalities: acid mine drainage on the Witwatersrand, South Africa. *The New South African Review*.

Fosso-Kankeu, E., 2018. Synthesized of-PFCl and GG-g-P(AN)/TEOS hydrogel composite used in hybridized technique applied for AMD treatment.. *Physics and Chemistry of the Earth*, 105, pp. 170-176.

Garland, R., 2011. Acid mine drainage – the chemistry. *Quest*, 07(02), pp. 50-52.

Gautam, R. K., Sharma, S. K., Mahiya, S. & Chattopadhyaya, M. C., 2014. *Contamination of Heavy Metals in Aquatic Media: Transport, Toxicity and Technologies for Remediation*. [Online]

Available at: <http://pubs.rsc.org/doi:10.1039/9781782620174-00001> [Accessed 06 June 2018].

Ghadimi, F., 2015. Prediction of heavy metals contamination in the groundwater of Arak region using artificial neural network and multiple linear regression. *Journal of Tethys*., 3(3), pp. 203–215.

Gholami , R., Kamkar-Rouhani , A., Ardejani , F. D. & Maleki, S., 2011. Prediction of toxic metals concentration using artificial intelligence techniques. *Applied Water Science*, Issue 01, pp. 125-134.

Gunatilake, S. K., 2015. Methods of Removing Heavy Metals from Industrial Wastewater. *Journal of Multidisciplinary Engineering Science Studies*, 01(01), pp. 12-19.

Heviánková, S. et al., 2013. Calcium Carbonate as an Agent in Acid Mine Water Neutralization. *Journal of the Polish Mineral Engineering Society*, pp. 160-168.

Heviánková, S. et al., 2013. Calcium Carbonate as an Agent in Acid Mine Water Neutralization. *Journal of the Polish Mineral Engineering Society*, pp. 160-168.

International Agency for Research on Cancer, 2014. IARC monographs on the evaluation of carcinogenic risks to humans. 1-115.

Jan, A. T., Azam , M., Siddiqui, K. & Ali, A., 2015. Heavy Metals and Human Health: Mechanistic Insight into Toxicity and Counter Defense System of Antioxidants. *International Journal of Molecular Sciences*, 16(1), p. 29592–29630.

Kefeni, K. K., Msangati, T. A. M. & Mamba, B. B., 2017. Acid mine drainage: Prevention, treatment options, and resource recovery: A review. *Journal of Cleaner Production*, 151(2017), pp. 475-493.

Khayatzadeh , J. & Abbasi , E., 2010. The Effects of Heavy Metals on Aquatic Animals. *The 1 st International Applied Geological Congress*, pp. 26-28.

Kirby, D., 2014. 'Effective Treatment Options for Acid Mine Drainage in the Coal Region of West Virginia', s.l.: the Graduate College of Marshall University.

Lehigh Earth Observatory EnviroSci, I., 2011. Overview of Chemicals Available to Treat AMD (Active). *Lehigh Environmental Initiative*, pp. 01.

LennTech, 1998-2020. *LennTech Water Treatment Solutions*. [Online] Available at: <https://www.lenntech.com/periodic/elements/si.htm#ixzz6QHgPo9na> [Accessed 24 06 2020].

LennTech, 2020. *water treatment processes*. [Online] Available at: <https://www.lenntech.com/processes/heavy/heavy-metals/heavy-metals.htm> [Accessed 04 06 2020].

Malik, Q. A. & Khan, M. S., 2016. Effect on Human Health due to Drinking Water Contaminated with Heavy Metals. *Journal of Pollution Effects & Control*, 5(1), pp. 1-2.

Marry Lissy, P. N. & Madhu, G., 2011. Removal of heavy metals from waste water using hyacinth. *Cochin University of Science and Technology*, 27(05), pp. 01.

Masindi , V., Chatzisyneon , E., Kortidis , I. & Foteinis, S., 2018. Assessing the sustainability of acid mine drainage (AMD ) treatment in South Africa. *Science of the Total Environment*, 635(01), pp. 793-802.

McCarthy, T. S., 2011. The impact of acid mine drainage in South Africa. *South African Journal of Science*, 107(5/6), pp. 1-7.

Moodely, I., Sheriden, C. M., Kappelmeyer, U. & Akcild, A., 2017. Environmentally sustainable acid mine drainage remediation: Research developments with a focus on waste/by-products. *Minerals Engineering*, pp. 1-14.

Nuttfeld, F., 2020. *Royal Society of Chemistry*. [Online] Available at: <https://edu.rsc.org/resources/neutralisation-curing-acidity/1756.article> [Accessed 06 07 2020].

Offeddu , F. G. et al., 2014. Processes affecting the efficiency of limestone in passive treatments for AMD: Column experiments. *Journal of Environmental Chemical Engineering*, 03(2015), pp. 304-316.

Olesik, J. W., Kinzer, J. A. & Harkleroad, B., 1994. Inductively Coupled Plasma Optical Emission Spectrometry Using Nebulizers with Widely Different Sample Consumption Rates. *Analytical Chemistry*, Volume 66, p. 13.

Peters , R. W. & Shem, L., 1998. Separation of heavy metals: removal from industrial wastewaters and contaminated soil. *Energy Systems Division Argonne National Laboratory*, pp. 01-64.

Rooki, R., Ardejani, F. D., Aryafar, A. & Asadi, A. B., 2011. Prediction of heavy metals in acid mine drainage using artificial. *Environ Earth Sci*, 64(1), pp. 1303–1316.

Roopali , R., Madhumita , R., Sufia , Z. & Abhijit, M., 2017. Bioaccumulation of heavy metals in Brassica juncea: an indicator species for phytoremediation. *International Journal For Innovative Research In Multidisciplinary Field* , 03(09), pp. 92.

Sadeghiamirshahidi , M., kish , T. E. & Ardejani, F. D., 2013. Application of artificial neural networks to predict pyrite oxidation in a coal washing refuse pile. *Elsevier Ltd.*, 103(01), pp. 163-169.

Sarkar, A. & Pandey, P., 2015. River Water Quality Modelling using Artificial Neural Network Technique. *Aquatic Procedia*, 04(01), pp. 1070-1077.

Sazli, M. H., 2006. A brief review of Feed-forward Neural Network. *Commun. Fac. Sci. Univ. Ank. Series A2-A3*, 50(01), pp. 11-17.

Science is fun in the laboratory of Shakhashira, 2017. *SciFun*. [Online] Available at: <http://www.scifun.org/CHEMWEEK/Lime2017.pdf> [Accessed 06 07 2020].

Sela, G., 2020. *Smart fertilizer management*. [Online] Available at: <https://www.smart-fertilizer.com/articles/sulfur/> [Accessed 14 04 2020].

Shah, A. I., 2017. *Heavy metal impact on aquatic life and human health- An overview*. Montréal, 37th Annual Conference of the International Association for Impact Assessment.

Stangroom, J., 2021. *Social Science Statistics- Linear Regression Calculator*. [Online] Available at: [https://www.socscistatistics.com/tests/regression/default.aspx#:~:text=The%20line%20of%20best%20fit%20is%20described%20by%20the%20equation,Y%20when%20X%20%3D%200\).](https://www.socscistatistics.com/tests/regression/default.aspx#:~:text=The%20line%20of%20best%20fit%20is%20described%20by%20the%20equation,Y%20when%20X%20%3D%200).) [Accessed 10 May 2021].

Toma, F. et al., 2004. Neural computation to predict TiO<sub>2</sub> photocatalytic efficiency for nitrogen oxides removal. *Journal of Photochemistry and Photobiology A: Chemistry*, 165(1-3), pp. 91-96.

Vlad, S., 2004. On the Prediction Methods Using Neural Networks Brief Overview of the ANNs. 01(01), pp. 01-06.

Water Specialists Technologies, L., 2020. *Water Specialists Technologies LLC*. [Online]  
Available at: [https://waterspecialists.biz/?page\\_id=115](https://waterspecialists.biz/?page_id=115)  
[Accessed 06 07 2020].



## Appendix A

SETP OIN T  
LABORATORIES



### Water Analysis Report

Sample name			RawAMD Sample 1	RawAMD Sample 2	Neutrilized AMD Sample 1	Neutrilized AMO Sample 2	
Sample date			2019/11/26	2019/11/26	2019/11/26	2019/11/26	
Sample container description			Plastic Container	Plastic Container	Plastic Container	Plastic Container	
Submission date			2019/12/02	2019/12/02	2019/12/02	2019/12/02	
Sample type			Water	Water	Water	Water	
Set Point ID			WAT/20/061 6-0001	WAT/20/061 6-0002	WAT/20/061 6-0003	WAT/20/051 6-0004	
Visual inspection			N/A	N/A	N/A	N/A	
Method no	Determinand	Unit					
Chemical Properties and Parameters							
M469	Chloride	mg/L	58.4	58.5	59.8	59.3	
M461	Conductivity	mS/m@2s•c	362	364	331	327	
M475	Fluoride	mg/L	0.80	0.90	<0.10	<0.10	
M465	Nitrate Nitrogen	mg/LN	<0.10	<0.10	0.27	0.37	
M466	Nitrite Nitrogen	mg/LN	<0.10	<0.10	<0.10	<0.10	
M460	pH	-	4.17	4.17	7.90	8.26	
M476	Sulphate	mg/L	1627	1634	1510	1520	
M463	Total Alkalinity	mg/LCaCO3	<10.0	<10.0	25.8	20.2	
M473	Total Dissolved Solids	mg/L@1so•c	2357	2370	2153	2127	
M474	Silver(Ag)	µg/L	<0.50	<0.50	<0.50	<0.50	
M474	Aluminium (Al)	mg/L	<0.15	<0.15	<0.15	<0.15	
M474	Arsenic (As)	µg/L	2.64	2.46	2.61	2.31	
M474	Barium (Ba)	µg/L	11.4	10.7	1.89	1.99	
M474	Beryllium (Be)	µg/L	<0.10	<0.10	<0.10	<0.10	
#	Bismuth (Bi)	mg/L	<0.10	<0.10	<0.10	<0.10	
M474	Calcium (Ca)	mg/L	683	709	872	856	
M474	Cadmium (Cd)	µg/L	0.19	0.17	<0.10	<0.10	
M474	Cobalt(Co)	µg/L	402	397	69.4	61.6	
M474	Chromium (Cr)	µg/L	<3.00	<3.00	<3.00	<3.00	
M474	Copper(Cu)	µg/L	7.26	6.42	11.4	11.0	
M474	Iron (Fe)	mg/L	289	289	<0.10	<0.10	
M474	Potassium (Kl	mg/L	19.5	20.3	20.8	20.4	
#	Lithium (Li)	mg/L	0.12	0.12	0.12	0.12	
M474	Magnesium (Mg)	mg/L	183	187	168	168	
M474	Manganese (Mn)	µg/L	45000	46500	53.3	50.2	
M474	Molybdenum (Mo)	µg/L	<1.00	<1.00	<1.00	<1.00	
M474	Sodium (Na)	mg/L	170	175	180	175	
#	Niobium (Nb)	mg/L	<0.02	<0.02	<0.02	<0.02	
M474	Nickel (Ni)	µg/L	521	490	27.2	20.3	
M474	Lead (Pb)	µg/L	<1.00	<1.00	<1.00	<1.00	



#	Sulphur(S)	mg/L	1243	1225	1093	1128	
M474	Antimony (Sb)	µg/L	<0.50	<0.50	0.54	0.52	
M474	Selenium (Se)	µg/L	2.71	2.63	2.90	2.61	
M474	Silicon (Si)	mg/L	8.56	8.58	0.37	0.38	
M474	Tin (Sn)	µg/L	<0.20	<0.20	<0.20	<0.20	
M474	Strontium (Sr)	µg/L	346	347	271	274	
#	Tantalum (Ta)	mg/L	0.02	<0.02	<0.02	<0.02	
#	Titanium (Ti)	mg/L	<0.04	<0.04	<0.04	<0.04	
M474	Vanadium (V)	µg/L	1.11	1.12	1.29	1.46	
M474	Zinc (Zn)	mg/L	0.33	0.36	0.07	0.08	
#	Zirconium (Zr)	mg/L	0.01	0.01	<0.01	<0.01	

Sample name			RAWAMDI	RAWAMD2	TREATEDAMD 1	TREATEDAMD 2	RAWAMDI	RAWAMD2	TREATEDAMD 1	TREATEDAMD 2	RAWAMDI	RAWAMD2	TREATEDAMD 1
Sample date			2020/03/13	2020/03/13	2020/03/13	2020/03/13	2020/03/16	2020/03/16	2020/03/16	2020/03/16	2020/03/18	2020/03/18	2020/03/18
Sample container description			2L Plastic Bottle	2L Plastic Bottle	2L Plastic Bottle	2L Plastic Bottle	2L Plastic Bottle	2L Plastic Bottle	2L Plastic Bottle	2L Plastic Bottle	2L Plastic Bottle	2L Plastic Bottle	2L Plastic Bottle
Submission date			2020/07/21	2020/07/21	2020/07/21	2020/07/21	2020/07/21	2020/07/21	2020/07/21	2020/07/21	2020/07/21	2020/07/21	2020/07/21
Sample type			Water	Water	Water	Water	Water	Water	Water	Water	Water	Water	Water
Set Point ID			WAT/21/0075-0001	WAT/21/0075-0002	WAT/21/0075-0003	WAT/21/0075-0004	WAT/21/0075-0005	WAT/21/0075-0006	WAT/21/0075-0007	WAT/21/0075-0008	WAT/21/0075-0009	WAT/21/0075-0010	WAT/21/0075-0011
Visual inspection			N/A	N/A	N/A	N/A	N/A	N/A	N/A	N/A	N/A	N/A	N/A
Method no	Determinand	Unit											
Chemical Properties and Parameters													
M469	Chloride	mg/L	52.3	52.7	53.0	53.8	53.0	52.5	53.3	54.1	52.1	52.0	53.7
M461	Conductivity	mS/m@25°C	487	489	371	374	487	485	385	388	478	472	365
M475	Fluoride	mg/L	<0.10	<0.10	<0.10	<0.10	<0.10	<0.10	<0.10	<0.10	<0.10	<0.10	<0.10
M465	Nitrate Nitrogen	mg/LN	<0.10	0.16	<0.10	0.11	0.25	0.16	0.29	0.11	0.16	0.16	0.10
M466	Nitrite Nitrogen	mg/LN	<0.10	<0.10	<0.10	<0.10	<0.10	<0.10	<0.10	<0.10	<0.10	<0.10	<0.10
M460	pH	.	2.66	2.64	8.69	8.81	2.64	2.65	8.34	BAS	2.66	2.62	9.00
M476	Sulphate	mg/L	1547	1565	1430	1437	1562	1556	1465	1482	1550	1544	1436
M463	Total Alkalinity	mg/LCaCO3	<10.0	<10.0	25.8	25.2	<10.0	<10.0	24.6	24.8	<10.0	<10.0	24.8
M473	Total Dissolved Solids	mg/L@180°C	3110	3130	2377	2397	3110	3103	2463	2480	3057	3027	2337
M474	Silver (Ag)	µg/L	<0.50	<0.50	<0.50	<0.50	<0.50	<0.50	<0.50	<0.50	<0.50	<0.50	<0.50
M474	Aluminium (Al)	mg/L	<0.15	<0.15	<0.15	<0.15	<0.15	<0.15	<0.15	<0.15	<0.15	<0.15	<0.15
M474	Arsenic (As)	µg/L	4.30	3.40	4.66	4.81	3.34	4.29	4.32	6.01	3.16	3.60	4.18
M474	Barium (Ba)	µg/L	15.8	11.8	2.65	2.75	11.2	12.9	2.32	3.39	13.1	15.6	3.26
M474	Beryllium (Be)	µg/L	0.18	0.12	<0.10	<0.10	0.08	0.12	<0.10	<0.10	0.13	0.20	<0.10
M474	Bismuth (Bi)	mg/L	<0.10	<0.10	<0.10	<0.10	<0.10	<0.10	<0.10	<0.10	<0.10	<0.10	<0.10
M474	Calcium (Ca)	mg/L	658	683	763	751	674	685	789	763	656	622	749
M474	Cadmium (Cd)	µg/L	0.22	0.18	<0.10	<0.10	0.20	0.25	<0.10	<0.10	0.25	0.30	<0.10
M474	Cobalt (Co)	µg/L	442	367	140	136	403	414	126	170	456	527	113
M474	Chromium (Cr)	µg/L	<3.00	<3.00	<3.00	<3.00	<3.00	<3.00	<3.00	<3.00	<3.00	<3.00	<3.00

M474	Copper (Cu)	µg/L	12.1	7.08	9.00	9.81	6.78	8.15	10.4	17.3	8.15	8.88	9.72
M474	Iron (Fe)	mg/L	37.7	41.1	<0.10	<0.10	38.8	38.3	<0.10	<0.10	41.3	35.4	<0.10
M474	Potassium (K)	mg/L	20.2	20.6	21.1	20.8	20.8	21.5	21.2	20.5	20.5	20.8	21.2
M474	Lithium (Li)	mg/L	0.12	0.12	0.12	0.12	0.12	0.13	0.12	0.12	0.12	0.12	0.12
M474	Magnesium (Mg)	mg/L	178	180	147	145	180	186	150	147	182	182	136
M474	Manganese (Mn)	µg/L	38200	39200	27.20	13.90	39300	39400	38.3	33.2	39400	39600	15.5
M474	Molybdenum (Mo)	µg/L	<1.00	<1.00	<1.00	<1.00	<1.00	<1.00	<1.00	<1.00	<1.00	<1.00	<1.00
M474	Sodium I(Na)	mg/L	153	156	162	157	158	163	158	153	154	155	157
M474	Niobium (Nb)	mg/L	<0.02	<0.02	<0.02	<0.02	<0.02	<0.02	<0.02	<0.02	<0.02	<0.02	<0.02
M474	Nickel (Ni)	µg/L	452	443	19.5	20.1	450	443	21.8	43.7	594	586	21.0
M474	Lead (Pb)	µg/L	<1.00	<1.00	<1.00	<1.00	<1.00	<1.00	<1.00	<1.00	<1.00	<1.00	<1.00
M474	Sulphur (S)	mg/L	965	990	879	865	983	1000	910	891	979	951	863
M474	Antimony (Sb)	µg/L	<0.50	<0.50	<0.50	<0.50	<0.50	<0.50	<0.50	<0.50	<0.50	<0.50	<0.50
M474	Selenium (Se)	µg/L	2.85	<2.00	2.31	2.13	<2.00	2.68	<2.00	2.61	2.00	2.39	<2.00
M474	Silicon (Si)	mg/L	9.48	9.46	0.49	0.47	9.52	9.86	0.57	0.54	9.38	9.54	0.46
M474	Tin (Sn)	µg/L	<0.20	<0.20	<0.20	<0.20	<0.20	<0.20	<0.20	<0.20	<0.20	<0.20	<0.20
M474	Strontium (Sr)	µg/L	440	359	312	320	389	394	311	426	381	432	292
M474	Tantalum (Ta)	mg/L	<0.02	<0.02	<0.02	<0.02	<0.02	<0.02	<0.02	<0.02	<0.02	<0.02	<0.02
M474	Titanium (Ti)	mg/L	<0.04	<0.04	<0.04	<0.04	<0.04	<0.04	<0.04	<0.04	<0.04	<0.04	<0.04
M474	Vanadium (V)	µg/L	1.63	1.20	1.27	1.43	1.09	1.01	1.69	1.84	0.91	0.87	1.65
M474	Zinc (Zn)	mg/L	0.28	0.16	<0.06	<0.06	0.18	0.18	<0.06	<0.06	0.19	0.20	<0.06
M474	Zirconium (Zr)	mg/L	<0.01	<0.01	<0.01	<0.01	<0.01	<0.01	<0.01	<0.01	<0.01	<0.01	<0.01
Sample name			TREATED AMD2	RAWAMD1	RAWAMD2	TREATED AMD1	TREATED AMD2	RAWAMD1	RAWAMD2	TREATED AMD1	TREATED AMD2	RAWAMD1	RAWAMD2
Sample date			2020/03/18	2020/03/20	2020/03/20	2020/03/20	2020/03/20	2020/03/23	2020/03/23	2020/03/23	2020/03/23	2020/03/25	2020/03/25
Sample container description			2L Plastic Bottle	2L Plastic Bottle	2L Plastic Bottle	2L Plastic Bottle	2L Plastic Bottle	2L Plastic Bottle	2L Plastic Bottle	2L Plastic Bottle	2L Plastic Bottle	2L Plastic Bottle	2L Plastic Bottle
Submission date			2020/07/21	2020/07/21	2020/07/21	2020/07/21	2020/07/21	2020/07/21	2020/07/21	2020/07/21	2020/07/21	2020/07/21	2020/07/21
Sample type			Water	Water	Water	Water	Water	Water	Water	Water	Water	Water	Water
Set Point ID			WAT/21/0075 0012	WAT/21/0075 0013	WAT/21/0075 0014	WAT/21/0075 0015	WAT/21/0075 0016	WAT/21/0075 0017	WAT/21/0075 0018	WAT/21/0075 0019	WAT/21/0075 0020	WAT/21/0075 0021	WAT/21/0075 0022
Visual inspection			N/A	N/A	N/A	N/A	N/A	N/A	N/A	N/A	N/A	N/A	N/A
Method no	Determinand	Unit											
Chemical Properties and Parameters													
M469	Chloride	mg/L	52.6	54.2	54.6	58.3	56.5	56.4	57.1	57	58.3	57.6	53.8
M461	Conductivity	mS/m @ 25°C	369	481	479	383	388	478	480	388	382	485	474
M475	Fluoride	mg/L	<0.10	<0.10	<0.10	<0.10	<0.10	<0.10	<0.10	<0.10	<0.10	<0.10	1.03
M465	Nitrate Nitrogen	mg/LN	0.1	<0.10	<0.10	<0.10	0.18	<0.10	<0.10	<0.10	0.11	<0.10	0.1
M466	Nitrite Nitrogen	mg/LN	<0.10	<0.10	<0.10	<0.10	<0.10	<0.10	<0.10	<0.10	<0.10	<0.10	<0.10
M460	pH	-	9	2.66	2.6	8.52	8.64	2.64	2.57	8.84	8.8	2.68	2.73
M476	Sulphate	mg/L	1418	1573	1558	1515	1518	1584	1602	1515	1487	1612	1573
M463	Total Alkalinity	mg/L CaCO3	24.8	<10.0	<10.0	25.6	24.4	<10.0	<10.0	24.8	24.8	<10.0	<10.0

M473	Total Dissolved Solids	mg/L @ 180°C	2367	3070	3067	2457	2477	3057	3070	2490	2443	3107	3037
M474	Silver (Ag)	µg/L	<0.50	<0.50	<0.50	<0.50	<0.50	<0.50	<0.50	<0.50	<0.50	<0.50	<0.50
M474	Aluminium (Al)	mg/L	<0.15	<0.15	<0.15	<0.15	<0.15	<0.15	<0.15	<0.15	<0.15	<0.15	<0.15
M474	Arsenic (As)	µg/L	4.53	2.94	3.12	3.73	3.87	3.05	2.85	4.97	4.71	2.60	2.38
M474	Barium (Ba)	µg/L	3.54	12.3	13.5	2.03	2.25	13.1	13.1	4.01	4.20	10.9	11.2
M474	Beryllium (Be)	l,lg/L	<0.10	0.12	0.13	<0.10	<0.10	0.13	0.12	<0.10	<0.10	0.12	0.11
M474	Bismuth (Bi)	mg/L	<0.10	<0.10	<0.10	<0.10	<0.10	<0.10	<0.10	<0.10	<0.10	<0.10	<0.10
M474	Calcium (Ca)	mg/L	719	621	627	687	753	644	666	790	788	672	683
M474	Cadmium (Cd)	µg/L	<0.10	0.24	0.27	<0.10	<0.10	0.24	0.22	<0.10	<0.10	0.17	0.15
M474	Cobalt (Co)	µg/L	121	440	456	113	113	455	443	121	117	419	366
M474	Chromium (Cr)	µg/L	<3.00	<3.00	<3.00	<3.00	<3.00	<3.00	<3.00	<3.00	<3.00	<3.00	<3.00
M474	Copper (Cu)	µg/L	11.3	6.95	8.28	9.7	10.4	7.76	6.95	16.1	15.6	5.90	6.80
M474	Iron (Fe)	mg/L	<0.10	39.6	39.8	<0.10	<0.10	37.8	37.3	<0.10	<0.10	38.7	69.2
M474	Potassium (Kl)	mg/L	20.6	19.5	19.9	18.2	19.7	20.1	20.3	20.7	20.4	20.3	20.3
M474	Lithium (Li)	mg/L	0.11	0.11	0.11	0.11	0.12	0.12	0.12	0.12	0.12	0.12	0.12
M474	Magnesium (Mg)	mg/L	130	173	176	152	156	180	183	147	148	184	187
M474	Manganese (Mn)	µg/L	6.76	39700	40000	15.9	16.1	40100	39500	26.2	27.3	40000	39000
M474	Molybdenum (Mo)	µg/L	<1.00	<1.00	<1.00	<1.00	<1.00	<1.00	<1.00	<1.00	<1.00	<1.00	<1.00
M474	Sodium (Na)	mg/L	151	144	147	144	154	156	158	158	159	155	152
M474	Niobium (Nb)	mg/L	<0.02	<0.02	<0.02	<0.02	<0.02	<0.02	<0.02	<0.02	<0.02	<0.02	<0.02
M474	Nickel (Ni)	µg/L	24.8	558	540	19.4	22.9	552	577	39.4	41.2	544	537
M474	Lead (Pb)	µg/L	<1.00	<1.00	<1.00	<1.00	<1.00	<1.00	<1.00	<1.00	<1.00	<1.00	<1.00
M474	Sulphur (S)	mg/L	840	949	952	831	887	949	974	902	900	989	1003
M474	Antimony (Sb)	µg/L	<0.50	<0.50	<0.50	<0.50	<0.50	<0.50	<0.50	<0.50	<0.50	<0.50	<0.50
M474	Selenium (Se)	µg/L	2.14	2.16	2.25	<2.00	<2.00	2.04	<2.00	2.73	2.47	<2.00	<2.00
M474	Silicon (Si)	mg/L	0.44	9.44	9.43	0.43	0.43	8.97	9.18	0.53	0.53	9.20	9.33
M474	Tin (Sn)	µg/L	<0.20	<0.20	<0.20	<0.20	<0.20	<0.20	<0.20	<0.20	<0.20	<0.20	<0.20
M474	Strontium (Sr)	µg/L	317	386	396	289	295	383	384	310	303	367	323
M474	Tantalum (Ta)	mg/L	<0.02	<0.02	<0.02	<0.02	<0.02	<0.02	<0.02	<0.02	<0.02	<0.02	<0.02
M474	Titanium (Ti)	mg/L	<0.04	<0.04	<0.04	<0.04	<0.04	<0.04	<0.04	<0.04	<0.04	<0.04	<0.04
M474	Vanadium (V)	µg/L	1.51	0.67	0.70	1.62	1.50	0.61	0.48	1.71	1.72	0.30	0.24
M474	Zinc (Zn)	mg/L	<0.06	0.23	0.22	<0.06	<0.06	0.17	0.14	<0.06	<0.06	0.20	0.15
M474	Zirconium (Zr)	mg/L	<0.01	<0.01	<0.01	<0.01	<0.01	<0.01	<0.01	<0.01	<0.01	<0.01	<0.01

Sample name		RawAMD1 Week3	RawAMD 2 Week3	Treated AMD1 Wi,i,k,3	Treated AMD2 \\A/u,k_3	RawAMD 1 Week4	RawAMD 2Week4	Treated AMD1 Week.4	Treated AMD2 \\A/ool,4	RawAMD 1 Week4	RawAMD 2 Week4	Treated AMD1 \\A/ook_4
Sample date		2020/04/01	2020/04/01	2020/04/01	2020/04/01	2020/04/03	2020/04/03	2020/04/03	2020/04/03	2020/04/06	2020/04/06	2020/04/06
Sample container description		2L Plastic Bottle	2L Plastic Bottle	2L Plastic Bottle	2L Plastic Bottle	2L Plastic Bottle	2L Plastic Bottle	2L Plastic Bottle	2L Plastic Bottle	2L Plastic Bottle	2L Plastic Bottle	2L Plastic Bottle
Submission date		2020/05/04	2020/05/04	2020/05/04	2020/05/04	2020/05/04	2020/05/04	2020/05/04	2020/05/04	2020/05/04	2020/05/04	2020/05/04
Sample type		Water	Water	Water	Water	Water	Water	Water	Water	Water	Water	Water

Set Point ID			WAT/20/0940-0001	WAT/20/0940-0002	WAT/20/0940-0003	WAT/20/0940-0004	WAT/20/0940-0005	WAT/20/0940-0006	WAT/20/0940-0007	WAT/20/0940-0008	WAT/20/0940-0009	WAT/20/0940-0010	WAT/20/0940-0011
Visual inspection			N/A	N/A	N/A	N/A	N/A	N/A	N/A	N/A	N/A	N/A	N/A
Method no	Determinand	Unit											
Chemical Properties and Parameters													
M469	Chloride	mg/L	47.3	47.6	48.7	48.8	48.1	48.3	48.9	49.3	48.1	48.0	48.9
M461	Conductivity	mS/m @ 25'C	314	315	305	303	315	314	306	310	311	312	301
M475	Fluoride	mg/L	1.10	1.43	<0.10	<0.10	1.76	1.62	<0.10	<0.10	1.73	0.96	<0.10
M465	Nitrate Nitrogen	mg/LN	<0.10	<0.10	<0.10	<0.10	<0.10	<0.10	<0.10	<0.10	<0.10	<0.10	<0.10
M466	Nitrite Nitrogen	mg/LN	<0.10	<0.10	<0.10	<0.10	<0.10	<0.10	0.10	<0.10	<0.10	<0.10	<0.10
M460	pH	-	4.16	4.17	8.60	8.61	4.10	4.21	8.60	8.67	4.12	4.14	8.96
M476	Sulphate	mg/L	1334	1344	1311	1318	1366	1374	1336	1332	1370	1370	1336
M463	Total Alkalinity	mg/LCaCO3	<10.0	<10.0	25.1	23.8	<10.0	<10.0	30.6	25.6	<10.0	<10.0	25.6
M473	Total Dissolved Solids	mg/L @ 180'C	2063	2057	1983	1973	2047	2043	1990	2013	2023	2030	1963
#	Silver (Ag)	mg/L	<0.01	<0.01	<0.01	<0.01	<0.01	<0.01	<0.01	<0.01	<0.01	<0.01	<0.01
M474	Aluminium (Al)	mg/L	<0.15	<0.15	<0.15	<0.15	<0.15	<0.15	<0.15	<0.15	<0.15	<0.15	<0.15
#	Arsenic (As)	mg/L	0.66	0.73	0.60	0.69	0.68	0.70	0.58	0.57	0.67	0.67	0.58
M474	Barium (Ba)	mg/L	0.01	0.Dl	<0.01	<0.01	0.01	0.01	0.00	0.00	0.Dl	0.Dl	0.01
M474	Beryllium (Be)	mg/L	<0.02	<0.02	<0.02	<0.02	<0.02	<0.02	<0.02	<0.02	<0.02	<0.02	<0.02
#	Bismuth (Bi)	mg/L	<0.10	<0.10	<0.10	<0.10	<0.10	<0.10	<0.10	<0.10	<0.10	<0.10	<0.10
M474	Calcium (Ca)	mg/L	666	673	929	890	677	683	877	886	722	743	918
M474	Cadmium (Cd)	mg/L	0.07	0.06	0.04	0.04	0.06	0.06	0.04	0.04	0.06	0.06	0.04
M474	Cobalt (Co)	mg/L	0.63	0.63	0.25	0.25	0.58	0.58	0.26	0.26	0.61	0.60	0.25
M474	Chromium (Cr)	mg/L	<0.05	<0.05	<0.05	<0.05	<0.05	<0.05	<0.05	<0.05	<0.05	<0.05	<0.05
M474	Copper (Cu)	mg/L	<0.10	<0.10	<0.10	<0.10	<0.10	<0.10	<0.10	<0.10	<0.10	<0.10	<0.10
M474	Iron (Fe)	mg/L	158	156	<0.10	<0.10	180	183	<0.10	<0.10	189	189	<0.10
M474	Potassium (K)	mg/L	17.1	18.1	18.4	19.2	18.4	18.3	19.3	19.3	18.5	18.2	19.4
#	Lithium (Li)	mg/L	0.11	0.12	0.11	0.12	0.12	0.12	0.12	0.12	0.12	0.12	0.12
M474	Magnesium (Mg)	mg/L	184	183	138	141	184	187	161	160	180	182	138
M474	Manganese (Mn)	mg/L	39.6	40.1	0.04	0.04	39.3	39.4	0.03	0.03	40.4	40.5	0.02
M474	Molybdenum (Mo)	mg/L	<0.02	<0.02	<0.02	<0.02	<0.02	<0.02	<0.02	<0.02	<0.02	<0.02	<0.02
M474	Sodium (Na)	mg/L	169	178	178	185	186	185	189	194	189	188	193
It	Niobium (Nb)	mg/L	<0.02	<0.02	<0.02	<0.02	<0.02	<0.02	<0.02	<0.02	<0.02	<0.02	<0.02
M474	Nickel (Ni)	mg/L	0.60	0.61	<0.02	<0.02	0.52	0.52	<0.02	<0.02	0.53	0.56	<0.02
It	Lead (Pb)	mg/L	0.12	0.D7	<0.05	0.06	0.11	0.17	0.09	<0.05	<0.05	0.05	<0.05
It	Sulphur (S)	mg/L	1103	1149	1151	1159	1141	1138	1188	1193	1221	1234	1189
It	Antimony (Sb)	mg/L	<0.02	<0.02	<0.02	<0.02	<0.02	<0.02	<0.02	<0.02	<0.02	<0.02	<0.02
It	Selenium (Se)	mg/L	0.08	<0.02	<0.02	0.Q7	<0.02	<0.02	<0.02	<0.02	0.04	<0.02	0.12
M474	Silicon (Si)	mg/L	7.41	7.64	0.81	0.81	8.04	7.91	0.52	0.51	8.49	8.55	0.59
It	Tin (Sn)	mg/L	0.08	0.10	0.12	0.06	<0.04	0.08	<0.04	0.06	0.06	0.18	0.11
M474	Strontium (Sr)	mg/L	0.34	0.35	0.28	0.29	0.35	0.35	0.27	0.27	0.36	0.36	0.31

#	Tantalum (Ta)	mg/L	<0.02	<0.02	<0.02	<0.02	<0.02	<0.02	<0.02	<0.02	<0.02	<0.02	<0.02
#	Titanium (Ti)	mg/L	<0.04	<0.04	<0.04	<0.04	<0.04	<0.04	<0.04	<0.04	<0.04	<0.04	<0.04
M474	Vanadium (V)	mg/L	<0.10	<0.10	<0.10	<0.10	<0.10	<0.10	<0.10	<0.10	<0.10	<0.10	<0.10
M474	Zinc (Zn)	mg/L	0.27	0.25	<0.06	<0.06	0.22	0.20	<0.06	<0.06	0.27	0.27	<0.06
M474	Zirconium (Zr)	mg/L	<0.01	<0.01	<0.01	<0.01	<0.01	<0.01	<0.01	<0.01	<0.01	<0.01	<0.01

Sample name		Treated AMD 2 Week4											
Sample date		2020/04/06											
Sample container description		2L Plastic Bottle											
Submission date		2020/05/04											
Sample type		Water											
Set Point ID		WAT/20/0940- 0012											
Visual inspection		N/A											
Method no	Determinand	Unit	Chemical Properties and Parameters										
M469	Chloride	mg/L	49										
M461	Conductivity	mS/m @ 25°C	300										
M475	Fluoride	mg/L	<0.10										
M465	Nitrate Nitrogen	mg/LN	<0.10										
M466	Nitrite Nitrogen	mg/LN	<0.10										
M460	pH	-	8.99										
M476	Sulphate	mg/L	1323										
M463	Total Alkalinity	mg/LCaCO3	21.2										
M473	Total Dissolved Solids	mg/L @ 180°C	1953										
#	Silver (Ag)	mg/L	<0.01										
M474	Aluminum (Al)	mg/L	<0.15										
#	Arsenic (As)	mg/L	0.64										
M474	Barium (Ba)	mg/L	0.01										
M474	Beryllium (Be)	mg/L	<0.02										
#	Bismuth (Bi)	mg/L	<0.10										
M474	Calcium (Ca)	mg/L	912										
M474	Cadmium (Cd)	mg/L	0.04										
M474	Cobalt (Co)	mg/L	0.26										



M474	Chromium {Cr}	mg/L	<0.05										
M474	Copper {Cu}	mg/L	<0.10										
M474	Iron {Fe}	mg/L	<0.10										
<b>M474</b>	Potassium {K}	mg/L	18.7										
#	Lithium {Li}	mg/L	0.11										

M474	Magnesium (Mg)	mg/L	139										
M474	Manganese (Mn)	mg/L	0.02										
M474	Molybdenum (Mo)	mg/L	<0.02										
M474	Sodium (Na)	mg/L	186										
#	Niobium (Nb)	mg/L	<0.02										
M474	Nickel (Ni)	mg/L	<0.02										
#	Lead (Pb)	mg/L	<0.05										
#	Sulphur (S)	mg/L	1155										
#	Antimony (Sb)	mg/L	<0.02										
#	Selenium (Se)	mg/L	<0.02										
M474	Silicon (Si)	mg/L	0.57										
#	Tin(Sn)	mg/L	<0.04										
M474	Strontium (Sr)	mg/L	0.30										
#	Tantalum (Ta)	mg/L	<0.02										
#	Titanium (Ti)	mg/L	<0.04										
M474	Vanadium (V)	mg/L	<0.10										
M474	Zinc (Zn)	mg/L	<0.06										
M474	Zirconium (Zr)	mg/L	<0.01										

Please Note:

N/A: Not applicable

RTF : Result to follow

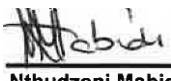
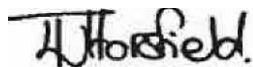
•sub-contracted Analysis

# Non SANAS Accredited methods.

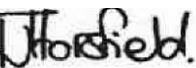
*Results only relate to the samples tested and are reported on an "as received" basis, unless otherwise specified. This report may not be reproduced, except in full, without the written approval of Set Point Laboratories; Results are subject to uncertainty of measurement, which are indicated on the enclosed information sheet.*

*While every effort is made to provide analysis of the highest accuracy, the liability of Set Point Laboratories is restricted to the cost of the analysis.*

#Comment:

  
Nthudzeni Mabidi

Nthudzeni Mabidi  
(Report Compiler)

  
\_\_\_\_\_  
Thelma Horsfield  
Technical Signatory

Moses Lelaka  
Technical Signatory

#Tests marked "Non SANAS Accredited method s", as well as any comments, opinions or interpretations expressed in this report are not

## INFORMATION SHEET TO ANALYSIS REPORT

### Methods used, tests subcontracted and accredited ranges:

DETERMINAND	Method code	Accredited	Ave. Uncertainty	Technique	Limit of Detection	Analytical range
pH	M460 / M860	Yes	13%	Electro-metric	03	4-10
Conductivity	M461 / M861	Yes	62%	Electro-metric	1 mS/m	1-1000mS/m
Alkalinity	M463 / M863	Yes	42%	Titration	10mg/L CaCO <sub>3</sub>	10 - 700 mg/l
Ammonia Nitrogen	M464	Yes	1:1 i % < 2.6 mg/L >2.4%	Automated Photometric	0.1 mg/L NH <sub>3</sub> -N	0.1 - 770 mg/L NH <sub>3</sub> -N
Ammonia Nitrogen	M864	Yes	1.8%	Automated Photometric	0.1 mg/L NH <sub>3</sub> -N	0.1 - 2.0 mg/L NH <sub>3</sub> -N
Nitrate Nitrogen	M465/M865	Yes	Calculated from M467 and M466 or M867 and M866	Automated Photometric	0.1 mg/L NO <sub>3</sub> -N	0.1 - 770 mg/L NO <sub>3</sub> -N
Nitrite Nitrogen	M466 / M866	Yes	118%	Automated Photometric	0.1 mg/L NO <sub>2</sub> -N	0.1 - 2.0 mg/L NO <sub>2</sub> -N
Nitrate and Nitrite Nitrogen	M467 / M867	Yes	12.5%	Automated Photometric	0.1 mg/L NO <sub>3</sub> +NO <sub>2</sub> -N	0.1 - 10 mg/L NO <sub>3</sub> +NO <sub>2</sub> -N
Ortho Phosphate	M468 / M868	Yes	7.2%	Automated Photometric	0.1 mg/L PO <sub>4</sub> -P	0.1 - 5 mg/L PO <sub>4</sub> -P
Chloride	M469 / M869	Yes	4.9%	Automated Photometric	3 mg/L Cl <sup>-</sup>	3 - 50 mg/L Cl <sup>-</sup>
Fluoride	M475/ M875	Yes	64%	Automated Photometric	0.1 mg/L F <sup>-</sup>	0.1 - 2 mg/L F <sup>-</sup>
Sulphate	M476/ M876	Yes	66%	Automated Photometric	3 mg/L SO <sub>4</sub>	3 - 100 mg/L SO <sub>4</sub>
Hexavalent Chromium	M471 / M871	Yes	30%	Automated Photometric	0.005 mg/L Cr <sup>6+</sup>	0.005 - 0.2 mg/L Cr <sup>6+</sup>
COD	M462 / M862	Yes	13%	Reflux/titrimetric	10 mg/L O <sub>2</sub>	10 - 1500 mg/L O <sub>2</sub>
Total Suspended Solids	M472 / M872	Yes	6.4%	Gravimetric	10 mg/L TSS	10 - 1500 mg/L TSS
Total Dissolved Solids	M473 / M873	Yes	1.5%	Gravimetric	10 mg/L TDS	10 - 1500 mg/L TDS
Al	M474 / M874	Yes	33%	ICP-OES	0.15 mg/L	0.15 - 15 mg/L
Ag	M474	Yes	0.32 ug/L	ICP-MS	0.50 ug/L	0.50 - 50 ug/L

As	M474/ M874	Yes	37%	ICP-OES	0 10 mg/L	0.10 - 15 mg/L
As	M474	Yes	Q 33 ug/L	ICP-MS	0 50 ug/L	0.50 * 50 ug/L
B	M474 / M874	Yes	44%	ICP-OES	0 35 mg/L	0 35-15 mg/L
Ba	M474 / M874	Yes	3.5 %	ICP-OES	0 01 mg/L	0 01 - 15 mg/L
Ba	M474	Yes	0 30 ug/L	ICP-MS	0 30 ug/L	0 30 - 100 ug/L
Be	M474/ M874	Yes	4 9%	ICP-OES	0 02 mg/L	002-15mg/L
Be	M474	Yes	0 37 ug/L	ICP-MS	0 10 ug/L	0.10 - 50 ug/L
Ca	M474/ M874	Yes	2 7 %	ICP-OES	0 50 mg/L	050-15mg/L

Cd	M474 I M874	Yes	4 5%	ICP-OES	a 02 mg/L	002-15mg/L
Cd	M474	Yes	a 36 ug/L	ICP-MS	a 10 ug/L	0.10 - 50 ug/L
Co	M474I M874	Yes	30%	ICP-OES	0 02 mg/L	a 02-15 mg/L
Co	M474	Yes	0 36 ug/L	ICP-MS	a 20 ug/L	a 20 - 50 ug/L
Cr	M474I M874	Yes	3 a%	ICP-OES	a as mg/L	a 05-15 mg/L
Cr	M474	Yes	a 36 ug/L	ICP-MS	3 a ug/L	3 -100 ug/L
Cu	M474 I M874	Yes	31 %	ICP-OES	a 10 mg/L	010-15mg/L
Cu	M474	Yes	a 36 ug/L	ICP-MS	1 a ug/L	1 - 100 ug/L
Fe	M474IM874	Yes	32%	ICP-OES	a 10 mg/L	010-15mg/L
Hg	M474	Yes	a 04 ug/L	ICP-MS	a so ug/L	050-Sug/L
K	M474 /M874	Yes	42%	ICP-OES	a 04 mg/L	004-15mg/L
Mg	M474 I M874	Yes	29%	ICP-OES	005 mg/L	a 05- 15 mg/L
Mn	M474/ M874	Yes	38%	ICP-OES	a 02 mg/L	0 02- 15 mg/L
Mn	M474	Yes	a 40 ug/L	ICP-MS	a 25 ug/L	025- 50 ug/L
Mo	M474 I M874	Yes	32 %	ICP-OES	a 02 mg/L	a 02-15 mg/L
Mo	M474	Yes	a 36 ug/L	ICP-MS	1 a ug/L	1 0 - 50 ug/L
Na	M474 / M874	Yes	77 %	ICP-OES	a 20 mg/L	0.20- 15 mg/L
Ni	M474/M874	Yes	30%	ICP-OES	0 02 mg/L	0 02- 15 mg/L
Ni	M474	Yes	0 33 ug/L	ICP-MS	1 a ug/L	10-100ug/L
Pb	M474 / M874	Yes	30 %	ICP-OES	a as mg/L	005-15mg/L
Pb	M474	Yes	a 37 ug/L	ICP-MS	1 a ug/L	10-100ug/L
Si	M474/ M874	Yes	68 %	ICP-OES	a 25 mg/L	025-15mg/L
Sb	M474	Yes	a 35 ug/L	ICP-MS	0 50 ug/L	a 50- 50 ug/L
Se	M474	Yes	a 35 ug/L	ICP-MS	2 0 ug/L	20-S0ug/L
Sn	M474	Yes	041 ug/L	ICP-MS	a 20 ug/L	a 20-so ug/L
Sr	M474 IM874	Yes	56%	ICP-OES	a 01 mg/L	001-15mg/L

Sr	M474	Yes	a 32 ug/L	ICP-MS	a so ug/L	a so - so ug/L
Th	M474	Yes	a 35 ug/L	ICP-MS	a 20 ug/L	0.20 - 50 ug/L
Tl	M474	Yes	a 29 ug/L	ICP-MS	a 10 ug/L	a 10- 50 ug/L
U	M474	Yes	a 30 ug/L	ICP-MS	a 20 ug/L	a 20- so ug/L
V	M474/M874	Yes	2.9%	ICP-OES	a 10 mg/L	0.10 -15 mg/L
V	M474	Yes	a 36 ug/L	ICP-MS	a 20 ug/L	0.20-50 ug/L
Zn	M474/ M874	Yes	49 %	ICP-OES	a 06 mg/L	0.06 • 15 mg/L

*Note: All other tests or elements reported are not accredited unless specified otherwise. Record: Analysis report information sheet, revision status: 2020-02-28*

Compiled and approved by: T Horsfield

